




Expression of growth arrest specific 1 (Gas1) in the distal tubules and collecting ducts in normal kidney and in the early stages of diabetic nephropathy

Brenda I. Luna-Antonio¹ · Rafael Rodríguez-Muñoz² · Carmen Namorado-Tonix² · Alejandro Pérez-López² · Elsa I. Sanchez² · Paula Vergara² · José L. Reyes² · José Segovia² 

Received: 20 February 2022 / Accepted: 15 September 2022 / Published online: 22 October 2022
© The Author(s), under exclusive licence to Springer Nature B.V. 2022

Abstract

The Growth Arrest-Specific protein 1 (Gas1) has been recently described in kidney as an endogenous inhibitor of cell proliferation in mesangial cells and with an important role in the maintenance of nephron progenitor cells. Furthermore, the expression of Gas1 was demonstrated in NCAM+ progenitor parietal cells of Bowman's capsule. Thus, the aim of this study was to analyze the expression of Gas1 in the collecting ducts (CD) of healthy rats and to examine whether high glucose levels modify its expression during the early stages of diabetes in STZ-treated rats. Immunofluorescence reveals that principal cells AQP2+ express Gas1 in both healthy and diabetic conditions. Western blot from enriched fractions of medullary CD suggests that diabetes promotes the increase of Gas1. AQP2+ cells are also positive for the expression of CD24 and CD1133 in diabetic rats. In addition, diabetes modifies the cell morphology in the CD and favors the increase of principal cells (AQP2+/Gas1+), induces a significant decrease of intercalated cells (V-ATPase+/Gas1-) and the presence of intermediate cells (Gas1+/V-ATPase+) which express both principal and intercalated cell markers. The expression of Gas1 in the distal tubules was also determined by immunofluorescence, western blot and ELISA in diabetic rats. The results identify Gas1 as a specific marker of principal cells in healthy and diabetic rats and suggest that diabetes promotes the expression of Gas1. Gas1 may have an important role in the maintenance and differentiation to principal cells in the CD during early stages of diabetes.

Keywords Gas1 · Collecting duct · Cell morphology · Diabetic nephropathy · AQP2

Introduction

Growth Arrest-Specific 1 (Gas1) is a plasma membrane protein with a glycosyl-phosphatidyl-inositol (GPI)-anchor with a molecular mass of approximately 37 kDa (Del Sal et al. 1994; Stebel et al. 2000). Gas1 is a pleiotropic protein implicated in several cellular and biological processes

including anti-proliferative and pro-apoptotic functions (Segovia and Zarco 2014). The over expression of Gas1 arrests cell proliferation through the inhibition of the DNA synthesis in the G₀ to S phase in NIH-3T3 fibroblasts and gliomas (Del Sal et al. 1992; Dominguez-Monzon et al. 2009; López-Ornelas et al. 2014). In neuroblastoma, hippocampal and glioma cells, the over-expression of Gas1 leads to cell death (Mellström et al. 2002; Zamorano et al. 2004; López-Ornelas et al. 2011; Zarco et al. 2012). Due to the capacity of Gas1 to trigger apoptosis, its potential role as a tumor suppressor in different tissues has been investigated (e.g. breast, liver, colorectal, and thyroid tumors) (Wang et al. 2012; Ma et al. 2013; Sacilotto et al. 2015; Li et al. 2016; Romero-Trejo et al. 2021). Gas1 is a negative modulator of the Glial cell-derived neurotrophic factor (GDNF) signaling inducing apoptosis by the activation of caspase 3 (Zamorano et al. 2003; Cabrera et al. 2006; López-Ramírez

✉ José Segovia
jsegovia@fsio.cinvestav.mx

¹ Departamento de Farmacología, Centro de Investigación y de Estudios Avanzados del IPN, Av. IPN #2508, 07360 Mexico City, México

² Departamento de Fisiología, Biofísica y Neurociencias, Centro de Investigación y de Estudios Avanzados del IPN, Av. IPN # 2508, 07360 Mexico City, Mexico

et al. 2008; Dominguez-Monzon et al., 2011; Zarco et al. 2012). During mouse development Gas1 has a positive participation in the Sonic Hedgehog (Shh) pathway acting as ligand-binding protein (Allen et al. 2007; Martinelli and Fan 2007). Furthermore, it was described that Gas1 is a target gene of the transcription factor C/EBP in granulosa cells in the ovary with a possible intervention in the ovulation and luteinization (Ren et al. 2016).

In the kidney, a study described the expression of Gas1 in SIX2 +nephron progenitor cells in the early stages of embryogenesis and it showed that the expression of Gas1 is modulated by the transcriptional factor WT1. Also, the expression of Gas1 during nephrogenesis was associated with the maintenance of a nephron progenitor cell population in the metanephric mesenchyme (Kann et al. 2015). In mature kidneys, the expression of Gas1 was described in the glomerulus, mainly in mesangial cells acting as an endogenous inhibitor of glomerular mesangial cells proliferation (van Roeyen et al. 2013). The expression of Gas1 is directly down-regulated by miR-34a in conditions of high glucose in vitro and in the early stages of diabetic nephropathy (DN) (Zhang et al. 2014). The expression of Gas1 was described in the parietal cells of Bowman's capsule and the co-expression with the renal progenitor cell marker NCAM; suggesting an important role for Gas1 in the differentiation of progenitor parietal cells of Bowman's capsule to podocytes in the early stages of diabetes (Luna-Antonio et al. 2017).

The collecting duct (CD) is a component of the distal nephron in the kidney with an important participation in the regulation of osmolarity and acid-base balance (Muto 2001). The CD possesses a heterogeneous cell morphology composed by two different types of epithelial cells: the principal and the intercalated cells, which perform different functions (O'Neil and Hayhurst 1985; Madsen and Tisher 1986; Holthofer et al. 1987). The principal cells are involved in sodium transport and water reabsorption by the epithelial sodium channel (ENaC) and the aquaporin 2 (AQP2) water channel while the intercalated cells are responsible for the regulation of acid-base homeostasis controlling proton secretion through the proton-pumping V-ATPase (Wagner et al. 2004; Brown et al. 2009; Ramkumar et al. 2014; Pearce et al. 2015; Roy et al. 2015; Jung and Kwon 2016). Diabetic nephropathy (DN) is a common complication of diabetes and it is considered the leading cause of end-stage renal disease. DN is characterized by persistent proteinuria, glomerular lesions, loss of glomerular filtration rate (GFR) and tubular alterations in diabetic patients (Habib 2013; Lim 2014). In rodent models of diabetes, hyperglycemia induces tubular cell hypertrophy and the increase of fluid content and pressure in the CD as well as an increased expression of cytokines and proteins related with interstitial fibrogenesis, like TGF- β , CTGF, SMA and VEGF (Wang et al. 2008).

Diabetes can induce impaired renal sodium excretion by proteolytic activation of ENaC and the presence of urine exosomes with AQP2 suggesting a damaged in the CD cells (Andersen et al. 2015).

The expression and function of Gas1 in the kidney has been only studied in glomerular cells. We studied the expression of Gas1 in the collecting duct cells and analyzed whether the high glucose condition during the early stages of diabetes modifies its expression. In addition, we explored the expression of Gas1 in the distal tubules.

Materials and methods

Reagents

The anti-human IgG Gas1 antibody was produced by ProSci (Poway, CA, USA). Anti-goat IgG Gas1 antibody was purchased from R&D Systems, Inc. (Minneapolis, MN, USA). Anti-goat IgG AQP2, anti-goat IgG CD24, anti-goat IgG claudin 8, anti-mouse IgG V-ATPase B1/2, anti-mouse IgG calbindin, anti-mouse IgG GAPDH antibodies were purchased from Santa Cruz Biotech, Inc. (Santa Cruz, CA, USA). Anti-mouse IgG claudins-2, -4, and -8, donkey anti-goat IgG Alexa Fluor 488, chicken anti-rabbit IgG Alexa Fluor 594, and donkey anti-mouse IgG Alexa Fluor 488 antibodies were purchased from Thermo Fisher Scientific (Waltham, MA, USA). Anti-rabbit IgG CD133 was purchased from Abcam (Cambridge, UK). Streptozotocin (STZ) was purchased from Sigma-Aldrich (St. Louis, Mo, USA).

Experimental design

Animal experiments were performed in accordance with the Mexican Official Norm NOM-062-ZOO-1999 and the Institutional Committee for the Care of Laboratory Animals (UPEAL) (protocol #491). Female Wistar rats with body weight of 200–250 g were housed with 12/12-h light/dark cycles at 22 ± 1 °C and $50 \pm 5\%$ humidity. All animals had access to food and water *ad libitum*. Type 1 diabetes was induced by the intraperitoneal (ip) administration of streptozotocin (STZ, 60 mg / kg body weight, single dose) diluted in citrate buffer, pH = 6.0. Non-diabetic control rats received only an intraperitoneal administration of citrate buffer. After 72 h, diabetes induction was confirmed. Blood glucose concentration was measured with the One Touch® Ultra blood glucose meter (Milpitas, CA, USA). Rats were sacrificed 7, 14 and 21 days after the induction of diabetes or vehicle administration.

Biochemical and physiological parameters

Glucose levels and body weight were monitored at 7, 14 and 21 days of diabetes. Rats were housed in metabolic cages 24 h prior to sacrifice. Urine samples were collected and volumes measured. Rats were deeply anesthetized with sodium pentobarbital (30 mg/kg, ip). Blood was collected by cardiac puncture and serum obtained. Urinary proteins were measured by the Lowry method (Bio-Rad Protein Assay Kit; Bio-Rad Laboratories, CA, USA). Creatinine clearance was measured by the modified Jaffé reaction as previously described (Hervey 1953; Luna-Antonio et al. 2017). Serum and urine samples were stored at -70 °C until use.

Extraction of renal tissues and total proteins from renal medulla

Kidneys from control and diabetic rats at 7, 14 and 21 days after the administration of STZ were perfused with isotonic saline solution (0.9% NaCl), excised and placed in ice-cold saline solution. Kidneys were decapsulated, and the renal medulla carefully isolated by microscopic dissection. To extract total protein, renal medulla was placed in ice-cold Krebs-Ringer bicarbonate solution (KRB) with 0.5 g/L bovine albumin, pH 7.4, osmolarity 290 mOsm/kg H₂O containing 15 mg of type II collagenase. Renal medulla was homogenized and washed three times with ice-cold KRB. Samples were incubated with the protease inhibitor cocktail Complete IX and phenylmethylsulfonyl fluoride (PMSF; 1 mM). The suspension was shaken at 4 °C and centrifuged. Pellets were suspended and incubated for 30 min at 4 °C in lysis buffer (RIPA). Samples were sonicated three times for 30 s in a high-intensity ultrasonic processor (Vibracell; Sonics & Materials, Inc., CT, USA) and centrifuged at 4 °C for 20 min, and supernatants were collected. Total protein quantification was performed using DC protein assay kit (Bio-Rad Laboratories, Hercules, CA, USA).

Isolation of distal tubules (DT)

DT were isolated by Percoll gradients as previously described (Reyes et al. 2002; Arreola-Mendoza et al. 2006; Molina-Jijón et al. 2014). Renal cortex was homogenized and placed in ice-cold KRB. Samples were suspended in KRB with 15 mg of collagenase Type II (Sigma-Aldrich Inc., St. Louis, MO), 10% bovine serum albumin and gassed with the appropriate mixture of 95% air/5% CO₂ in a shaking water bath for 20 min at 37 °C. Samples were incubated with ice-cold KRB solution with protease inhibitor cocktail Complete IX and PMSF. Collagen fibers in the samples were removed by filtering the suspension and the samples were centrifuged. Pellets were resuspended in bovine serum

albumin (5%) with protease inhibitors for 5 min at 4 °C and centrifuged, the supernatant was discarded. Pellets were suspended in ice-cold Percoll and KRB. Suspension was centrifuged (107 x g/30 min), resulting in the separation into four distinct bands. The first fraction on top of the Percoll gradient, was enriched in DT, and the fourth fraction on the bottom was enriched in proximal tubules. The second and third fractions in the middle of the Percoll gradient contained a mix of the nephron segments (including glomeruli, proximal tubules, and DT). All fractions were analyzed by light microscopy to confirm the morphological characteristics of each tubular segment.

Western blot analysis

Western blot was performed as previously described (Luna-Antonio et al. 2017; Rosas-Martínez et al. 2021). Samples were denatured by boiling for 12 min, and proteins loaded onto 10% SDS-PAGE gels and ran. Molecular weight standards (Amersham Pharmacia Biotech, Piscataway, NJ, -USA) were run in parallel. Proteins were transferred to polyvinylidene fluoride membranes (Amersham Bioscience, Uppsala, Sweden). Membranes were incubated with casein 3X (VECTOR, sp-5020; Burlingame, CA, USA) to block nonspecific protein binding. Membranes were incubated overnight at 4 °C with the primary antibodies against Gas1, CLND4, AQP2, CD24, CD133, V-ATPase and CLDN8 (dilution 1:500), previously indicated. Next, membranes were incubated with peroxidase-conjugated antibodies (dilution 1:10,000) for 1 h. The ECL Prime Western Blotting detection reagent (Amersham™, GE Healthcare, Buckinghamshire, UK) were used to develop immunoblots. To detect chemiluminescence, the EC3 Imaging System (UVP Bioimaging Systems, Cambridge, UK) was used. Protein density band was quantified by densitometry (UVP BioImaging Systems Software).

Medullary collecting ducts dissection

Renal medullary collecting tubules were isolated as previously described (Reyes et al. 1992; Gonzalez-Mariscal et al. 2000). Briefly, animals were sacrificed and kidneys immediately removed and placed in ice-cold KRB. Sections (1–2 mm) were cut along the corticomedullary axis from the isolated kidneys. Kidney sections were maintained in ice-cold KB at 4 °C, pH 7.4, gassed with 95% air/5% CO₂ during dissection. Collecting tubules were dissected and identified with a stereoscopic microscope (X20). Immunofluorescence was performed in dissected CD. Tubules were washed with PBS + Ca²⁺ (0.1 M) three times and fixed for 1 min with ice-cold ethanol (95%) and until evaporation with acetone at room temperature. Fixed tubules were

washed three times with PBS+Ca²⁺ and incubated with 0.2% Triton X-100 (Bio-Rad Laboratories, Hercules, CA, USA). Thereafter, tubules were washed with PBS+Ca²⁺ and blocked with 0.5% IgG-free bovine serum albumin for 30–40 min (1331-A, Research Organics Cleveland, OH, USA). The immunofluorescence protocol was performed maintaining the tubules at 4 °C.

Rat kidney frozen sections

Kidneys from control and diabetic groups were obtained and prepared as previously described (Gonzalez-Mariscal et al. 2000; Molina-Jijón et al. 2015). Kidney Sect. (4 µm) were cut with a Leica CM1100 cryostat (Heidelberg, Germany) and mounted on gelatin-coated slides. All samples were stored at -70 °C. For immunofluorescence experiments, the sections were fixed with methanol at -20 °C. Sections were hydrated with PBS and permeabilized with 0.2% Triton X-100. Subsequently, the sections were washed thrice with PBS and blocked with 0.5% IgG-free bovine serum albumin for 1 h.

Immunofluorescence

Frozen sections and dissected CD were incubated overnight at 4 °C with the following primary polyclonal antibodies: anti-human IgG Gas1, anti-goat IgG CD24, anti-rabbit IgG CD133 (dilution 1:100), anti-goat IgG CLDN8 and anti-goat IgG AQP2 (dilution 1:200), and the primary monoclonal antibodies: anti-mouse IgG V-ATPase and anti-mouse IgG calbindin (dilution 1:100). Next, incubation with the secondary antibody was performed for 2 h at room temperature. The secondary antibodies employed were: donkey anti-goat IgG Alexa Fluor 488, chicken anti-rabbit IgG Alexa Fluor 594, and donkey anti-mouse IgG Alexa Fluor 488 antibodies (dilution 1:100). To test the specificity of the primary antibody to Gas1, the expression of Gas1 in the CD was analyzed using different primary antibodies and comparing the expression in the tubular structure. The absence of Gas1 signal in the proximal tubules was considered as a negative control. To test the specific binding of the secondary antibodies, immunofluorescence with the primary antibodies in the absence of the corresponding secondary antibodies was performed.

Image acquisition

Confocal images were acquired using a confocal laser scanning microscope (TCS-SP8, Leica Microsystems, Heidelberg, Germany) mounted on an inverted microscope (DMI6000 Leica Microsystems, Heidelberg, Germany) equipped with diode (405 nm), OPAL (488 nm) OPAL

(552 nm) and diode (638 nm) lasers and 10x/0.40 IMM CS, 20x/0.75 IMM Corr CS2, 40x/1.30 Oil CS2 40x/1.10 and 63x/1.40 Oil CS objective (Leica Microsystems, Heidelberg, Germany). Image acquisition was performed with the LAS X Life Science Software (Leica Microsystems, Heidelberg, Germany) with XYZ scan mode, 900 gain, 1.0 µm pinhole diameter, pixels dimension 1024 × 1024, 400 Hz scan speed with bidirectional X, -33.48 phase X, image size 160.46 µm x 160.46 µm, pixel size 156.86 nm x 156.86 nm, zoom factor 1, Z-stack 19.7 µm and 23–67 steps/sections. Regions of interests were selected from the scan images, scale bars are shown in figure legends. Co-localization analysis was performed as previously described (Dunn et al. 2011; Moser et al. 2017). Co-localization was analyzed using the FIJI version (<http://fiji.sc>) of the free software ImageJ for processing images. Coloc2 plugin was used to calculate the Pearson's coefficient correlation and to obtain the 2D intensity histogram between two channels. The analysis was done in original, unmodified images.

Enzyme-linked immunosorbent assay of Gas1 in distal tubules

Protein extraction was performed as previously described (Ayala-Sarmiento et al. 2016; Estudillo et al. 2016). Gas1 protein was measured with an enzyme-linked immunosorbent

assay (ELISA) using the mouse Gas1 DuoSet ELISA Development kit (R&D Systems, Minneapolis, USA) according to the manufacturer's instructions. Data obtained were analyzed and normalized to obtain the amount of Gas1 protein in picograms per microgram protein.

Quantification of cell type in the collecting duct

A minimum of 3 dissected CD were analyzed to determine the average number of principal, intercalated and intermediate cells per tubule per rat (Mukherjee et al. 2019). Cells expressing AQP2+/Gas1+ were counted as principal, cells only expressing V-ATPase+/Gas1- were counted as intercalated, and cells expressing both AQP2+ and V-ATPase+ were counted as intermediate cells. Quantification of positively stained cells was evaluated using a confocal inverted microscope (TCS-SP8 Leica, Heidelberg, Germany) and the ImageJ software.

Data analysis

Results are expressed as means ± standard deviation (SD). Analysis of variance (ANOVA) was used for multiple comparisons among groups; followed by a *post hoc* Dunnett's test. *p* < 0.05 was considered statistically significant.

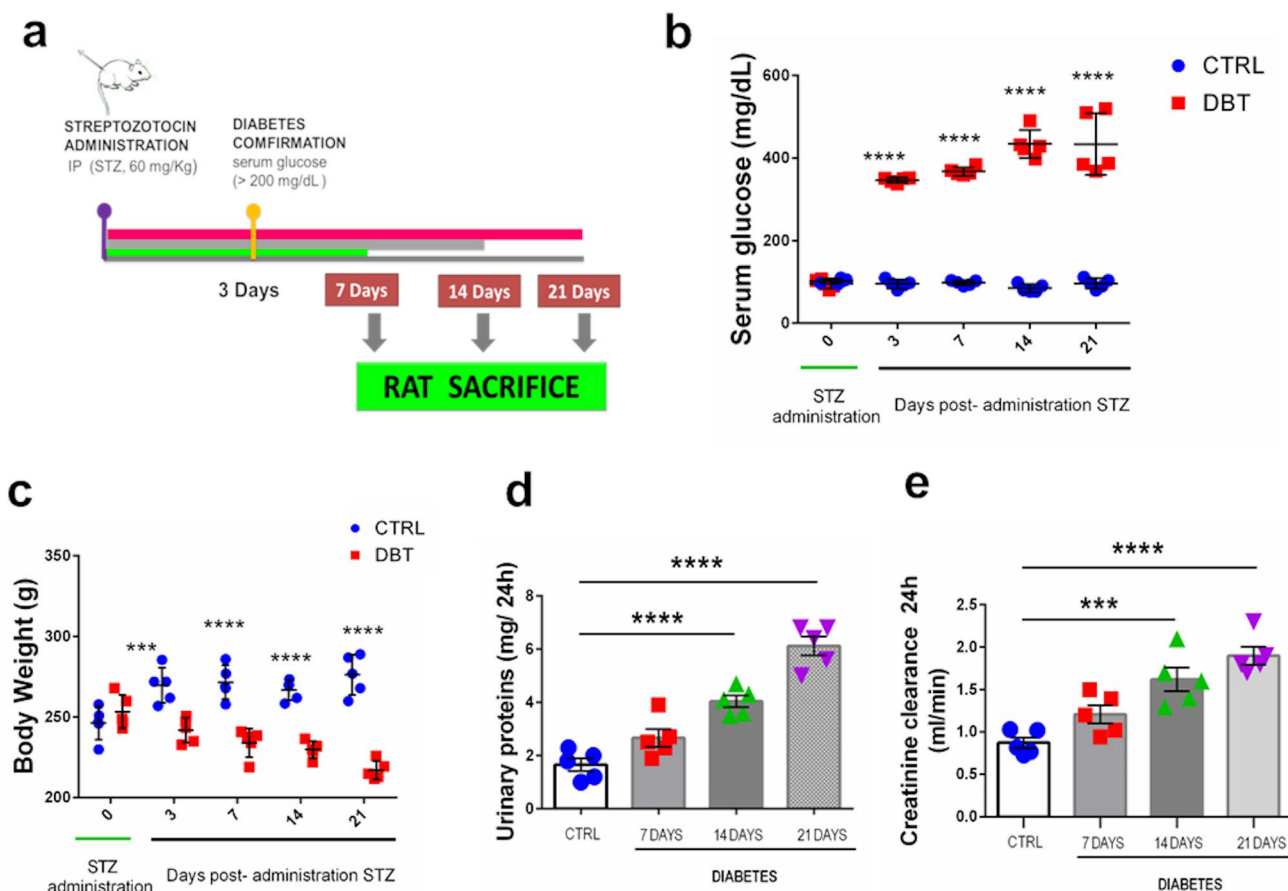


Fig. 1 Physiological and biochemical parameters in diabetic rats. **a** Type 1 diabetes was induced in Wistar rats by the intraperitoneal administration of streptozotocin (STZ) (60 mg / kg body weight, single dose). Three days after the administration of STZ, blood glucose concentration was measured to confirm the induction of diabetes. Rats were sacrificed 7, 14 and 21 days after the induction of diabetes or vehicle administration. **b-c** Serum glucose levels and body weight were monitored at 7, 14 and 21 days after STZ-administration. Rats

treated with STZ showed hyperglycemic indexes starting at 3 days until 21 days post STZ administration compared with controls. Diabetic rats treated with STZ showed a decrease in body weight compared with controls. **d** We also analyzed creatinine clearance and e urinary proteins. In both parameters we observed a gradual increase in the first 7 days with diabetes but it was not until the 14 and 21 days of diabetes that a significant increase was observed. Control (CTRL), diabetes (DBT). Values are in mean \pm standard deviation (SD), * $p < 0.05$, ** $p < 0.01$, *** $p < 0.001$, **** $p < 0.0001$, $n = 3$

Results

Induction of experimental diabetes and renal alterations

To confirm the induction of experimental diabetes in rats, blood glucose was determined in experimental groups and controls (Fig. 1a). Experimental groups treated with STZ exhibited high blood glucose (hyperglycemic index) within the first 3 days and up to the 21 days post STZ administration compared with controls (Fig. 1b). Body weight was also analyzed in diabetic rats at 7, 14 and 21 days after STZ and in control rats (Fig. 1c). A significant loss of body weight in diabetic rats was observed compared with control rats. To analyze renal function, proteinuria and creatinine

clearance were measured in diabetic groups at 7, 14 and 21 days after STZ and in control groups. (Fig. 1d-e). Both renal function parameters showed a progressive increase in diabetes, with a significant increase at 14 and 21 days of diabetes compared with controls. Our results show that diabetic rats present characteristics such as hyperglycemic indexes, body weight loss and alterations in renal function similar to human diabetes. Diabetic rats exhibited urinary protein excretion and hyperfiltration, both important features in the early stages of diabetic nephropathy (Campbell et al. 2003; Meeme and Kasozi 2009; Jerums et al. 2010; Palatini 2012; Trevisan and Dodesini 2017).

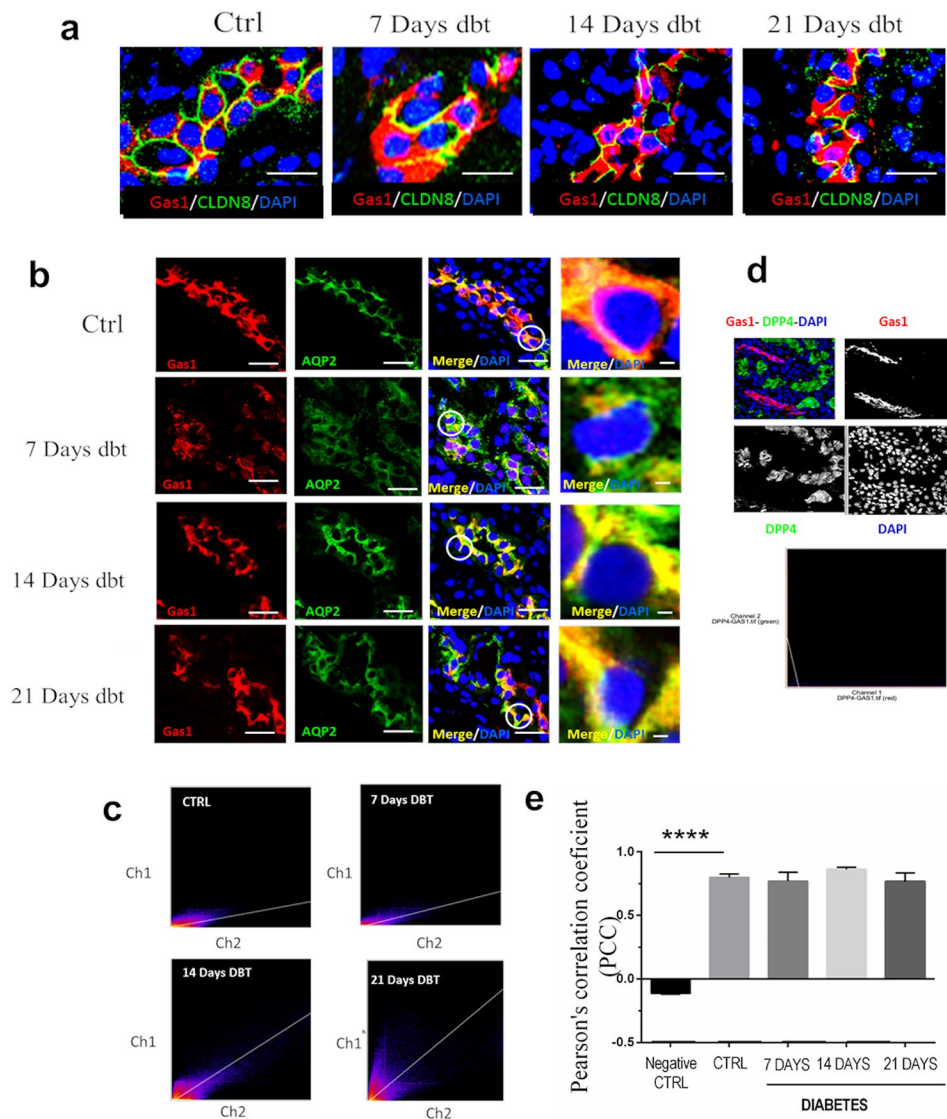


Fig. 2 Gas1 is expressed in the collecting duct in control rats and during the early stages of diabetes. **a** The expression of claudin-8 (CLDN8) and Gas1 was analyzed by immunofluorescence in kidney sections of healthy and diabetic rats at 7, 14 and 21 days. CLDN8 was used to identify the collecting ducts. In controls and in the diabetic rats of 7, 14 and 21 days Gas1 is expressed in the same tubular structure positive for CLDN8. We observed the expression of Gas1 in the cell membrane and in the cytoplasm in both conditions. **b** To evaluate the expression of Gas1 in the principal cells of the collecting duct, the expression of Gas1 and AQP2 was analyzed by immunofluorescence in healthy and in diabetic rats of 7, 14 and 21 days. Co-localization of Gas1 and AQP2 (yellow zones) in healthy and in the diabetic rats was observed.

Expression of Gas1 in the collecting ducts in healthy and diabetic rats treated with STZ

As shown (Supplementary Fig. 1), Gas1 expression is detected in the medulla both in healthy rats and in diabetic rats at 7, 14 and 21 days. In order to explore whether the

In the magnifications we observed the co-localization of Gas1+/AQP2+ in detail. **c** Co-localization analysis for Gas1 and AQP2. **d** Expression of Gas1 in the proximal tubule as negative control of co-localization. Immunofluorescence of Gas1 and the specific marker of proximal tubules dipeptidyl peptidase 4 (DPP4) was presented. **e** Pearson's coefficient correlation (PCC) for Gas1 and AQP2. Gas1+ (red), CLDN8+ (green), AQP2+ (green) and DAPI+ (blue). White circles indicated magnifications of Gas1+/CLDN8+ cells. Control (Ctrl); diabetes (dbt). Scale bars a = 40 μ m, b = 40 μ m and magnifications 28 μ m. Values are in mean \pm standard deviation (SD), * $p < 0.05$, ** $p < 0.01$, *** $p < 0.001$, **** $p < 0.0001$. All the experiments were performed in kidney sections. A representative experiment is shown (n = 3)

expression of Gas1 corresponds to the medullary CD, the expression of Gas1 and Claudin-8 (Cldn8) (Hou 2016) was analyzed by immunofluorescence in kidney sections of healthy and diabetic rats of 7, 14 and 21 days (Fig. 2a). The results show that both proteins are in the same tubular structure in the healthy and diabetic rats. The expression of Gas1 was detected in the cell membrane and in the cytoplasm in

both conditions. These results suggest that CD cells express Gas1.

The expression of Gas1 in kidney sections of healthy rats was analyzed by immunofluorescence using two different antibodies (Supplementary Fig. 2a). Claudin-4 and -8 were used as markers of CD (Hou 2016). In both experiments, the expression of Gas1 along the tubular structure was observed. Gas1 and Cldn-4 and -8 co-localized in both experiments. The results confirm that Gas1 is expressed in the CD. Background autofluorescence was not detected (Supplementary Fig. 2b). As a negative control, the expression of Gas1 in the proximal tubules was studied (Supplementary Fig. 2c). The expression of Gas1 and dipeptidyl peptidase-4 (DPP4), a specific marker of proximal tubules (Girardi et al. 2004), was analyzed by immunofluorescence. Gas1 and DPP4 are not localized in the same renal tubule in control rats nor in diabetic rats.

Principal cells of collecting ducts express Gas1 in healthy rats and diabetic rats treated with STZ

The pattern of expression of Gas1 is heterogeneous among cells in the CD, some cells express Gas1 and others are negative for the expression of Gas1 in both healthy and diabetic rats (Fig. 2a). The CD are characterized by possessing principal and intercalated cells; it is possible that Gas1 is only expressed in one cell type along the CD. To analyze if the principal cells express Gas1, immunofluorescence assays were performed in kidney sections to determine the expression of Gas1 and AQP2 (Fig. 2b). Gas1 and AQP2 co-localize (yellow zones) in healthy and diabetic rats at 7, 14 and 21 days of diabetes. Pearson's correlation coefficient (PCC) indicates a strong co-localization between Gas1 and AQP2 in healthy rats and diabetic rats at 7, 14 and 21 days (Fig. 2c-e). The expression of Gas1 and AQP2 was analyzed on the dissected CD by immunofluorescence (Fig. 3a) to confirm the previous results. Gas1 and AQP2 co-localize (yellow zones) along the tubular structure in both control and in the diabetic conditions. Quantitative co-localization analysis also shows a high overlapping of both proteins in healthy and diabetic groups (Fig. 3b-d). To observe in detail the tubular structure, the isolated tubules are shown in a bright field (Supplemental Fig. 3a). All the results show that the principal cells of the CD express Gas1 in normal conditions and during early stages of diabetes.

Expression of Gas1 in the intercalated cells of the collecting duct in healthy and diabetic rats

The expression of Gas1 and of V-ATPase was analyzed by immunofluorescence in kidney sections of healthy and diabetic rats (Fig. 4). V-ATPase+ cells do not express Gas1 in neither the healthy nor the diabetic rats. Low values of PCC (Fig. 4b-c) in healthy rats (Ctrl) suggesting a weak co-localization of Gas1 and V-ATPase (Ctrl, $PCC=0.193\pm 0.015$). In the diabetic rats (DBT) of 7, 14 and 21 days, a slight increase in PCC values was observed (7 days DBT, $PCC=0.343\pm 0.115$; 14 days DBT, $PCC=0.25\pm 0.04$ and 21 days DBT, $PCC=0.25\pm 0.02$). An immunofluorescence analysis of Gas1 and V-ATPase was performed in isolated CD for a detailed examination. In healthy rats, a well-defined "salt and pepper" distribution of Gas1 and V-ATPase proteins along the CD was observed. Although both proteins are expressed in the same tubular structure, they are not in the same cell type. The result suggests that intercalated cells do not express Gas1 in the healthy rats. At 7, 14 and 21 days of diabetes, most V-ATPase+ cells do not express Gas1 as was observed in healthy rats. Interestingly, few cells that expressed both proteins (Gas1+/V-ATPase+) were observed in the diabetic condition (Fig. 6 white arrows and Supplementary Fig. 4). These cells were identified as intermediate cells. A quantitative co-localization analysis of Gas1 and V-ATPase was performed in the isolated CD to confirm the results. A weak co-localization of Gas1 and V-ATPase in healthy rats was observed (Ctrl, $PCC=0.25\pm 0.035$). However, in diabetic rats a significant increase in the PCC values was found (7 Days DBT, 0.58 ± 0.06 ; 14 Days DBT, 0.69 ± 0.070 ; 21 Days DBT, 0.73 ± 0.035), suggesting a moderate co-localization of Gas1 and V-ATPase in the diabetic conditions. To observe in detail the tubular structures, the isolated CDs are shown in the bright field (Supplemental Fig. 3b). The results suggest that intercalated cells of the CD do not express Gas1 in healthy, nor in diabetic rats. Moreover, diabetes favors the appearance of some cells that express Gas1 and V-ATPase (intermediate cells) in the CD.

Diabetes favors the decrease of intercalated V-ATPase⁺/Gas1⁻ cells and the presence of Gas1⁺/V-ATPase⁺ intermediate cells in the collecting ducts

The quantification of principal cells Gas1+/AQP2+, intercalated cells V-ATPase+/Gas1- and intermediate cells Gas1+/V-ATPase+ was performed in isolated CD of healthy and diabetic rats to identify the cell population (Fig. 7). In the first 7 days of diabetes a significant increase of AQP2+/

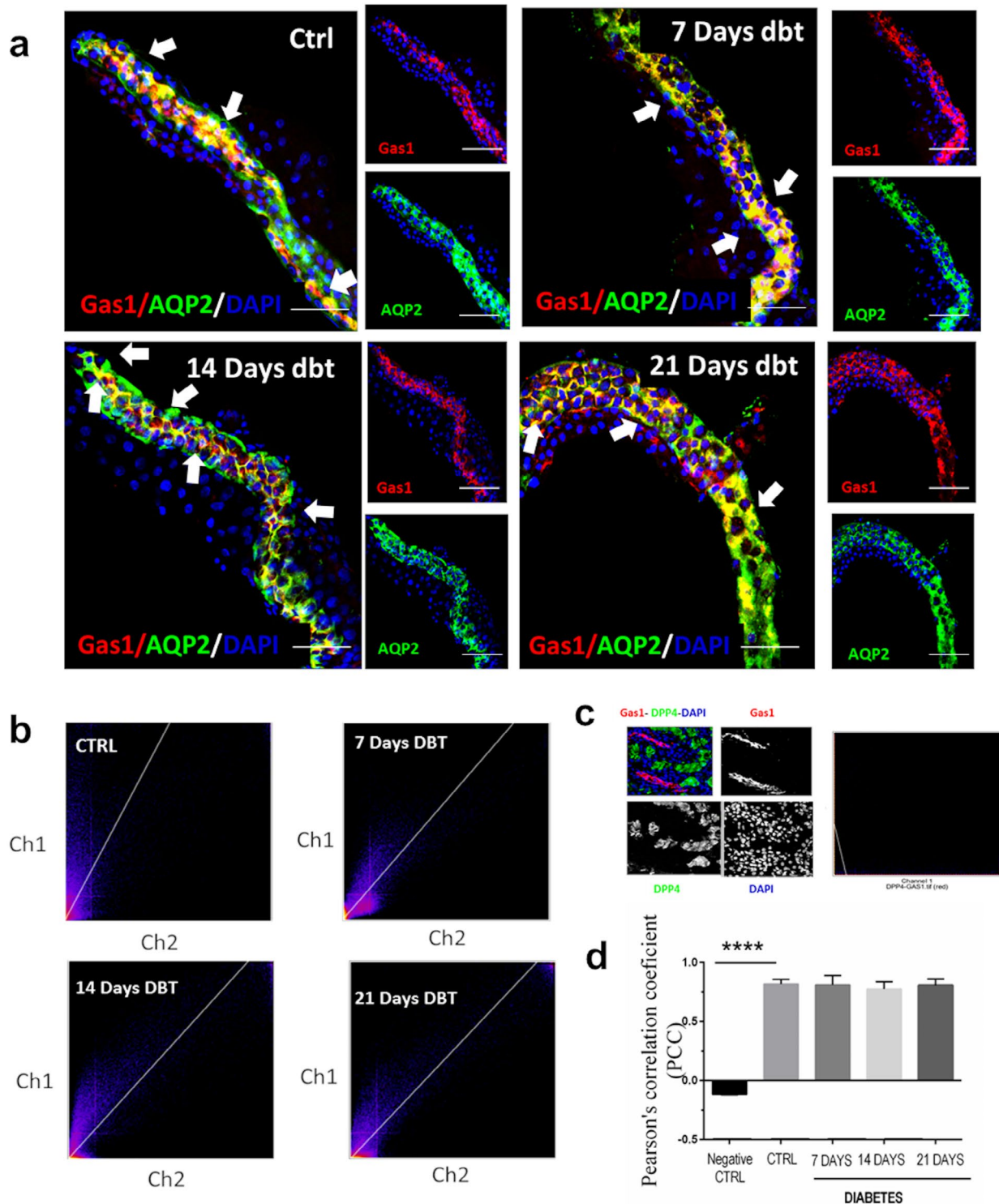


Fig. 3 Gas1 is expressed in the principal cells of the collecting duct. **a** To determine the expression of Gas1 in the principal cells a manual dissection of collecting ducts in healthy and diabetic rats was performed. Expression of Gas1 and AQP2 was analyzed by immunofluorescence in dissected collecting ducts. Co-localization of Gas1 and AQP2 (white arrows) was observed in healthy and diabetic rats of 7, 14 and 21 days of diabetes. **b** Co-localization analysis for Gas1 and AQP2. **d** Expression of Gas1 in the proximal tubule as negative

control of co-localization. Immunofluorescence of Gas1 and the specific marker of proximal tubules dipeptidyl peptidase 4 (DPP4) is presented. **d** Pearson's coefficient correlation (PCC) for Gas1 and AQP2. Gas1+ (red), AQP2+ (green) and DAPI+ (blue). White arrows indicate Gas1+ /AQP2+ cells (yellow). Control (Ctrl); diabetes (dbt). Scale bar, 30 μm. Values are in mean ± standard deviation (SD). * $p < 0.05$, ** $p < 0.01$, *** $p < 0.001$, **** $p < 0.0001$. All the experiments were performed in isolated renal tubules. A representative experiment is shown ($n = 3$)

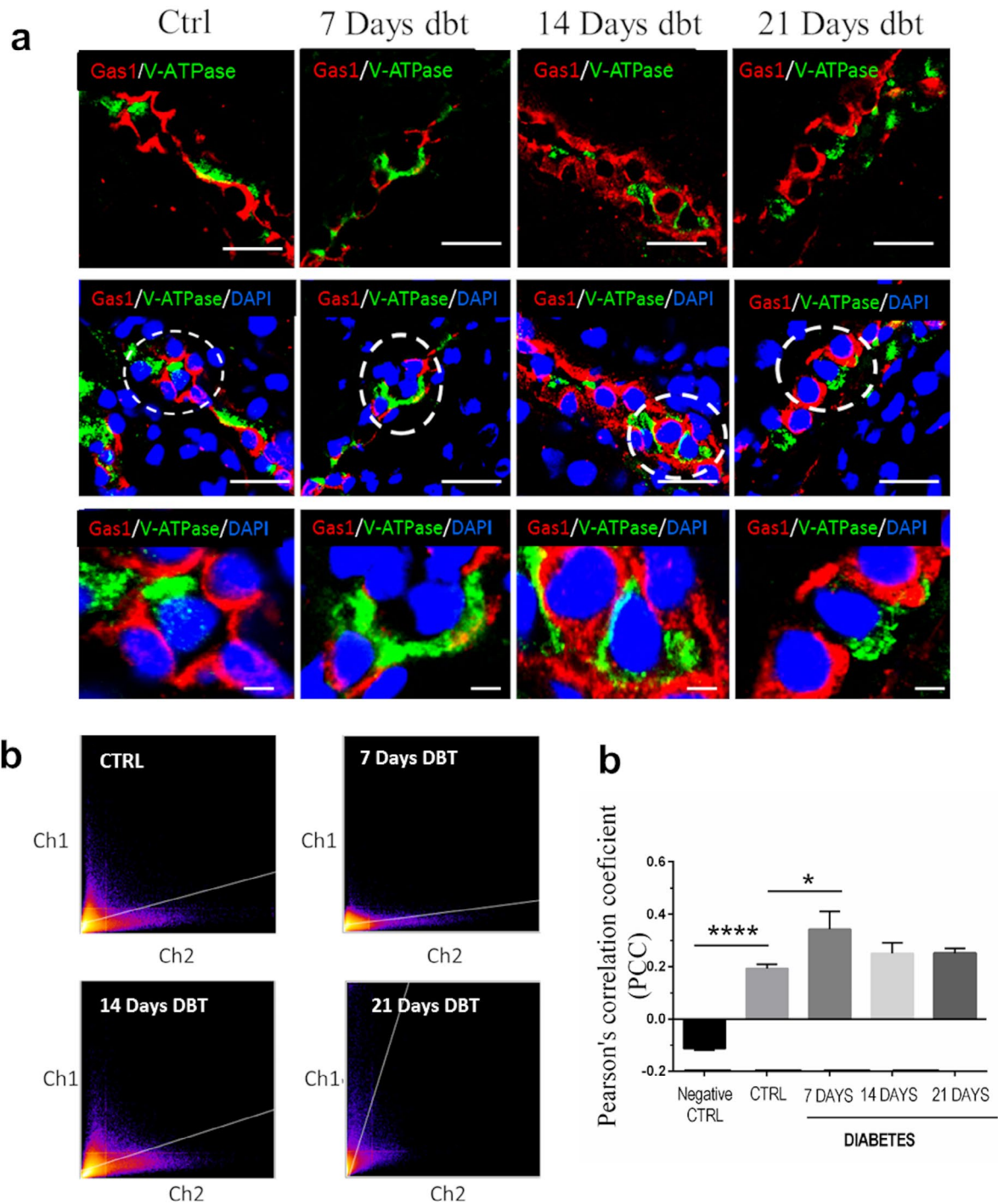


Fig. 4 The intercalated cells do not express Gas1 in the early stages of diabetes. **a** Analysis by immunofluorescence of Gas1 and V-ATPase (intercalated cell marker). Immunofluorescence was performed in kidney sections in healthy and diabetic rats of 7, 14 and 21 days. Gas1 and V-ATPase did not co-localize in either conditions. In the magnifications we observed that in most of the tubules, intercalated cells V-ATPase+ are surrounded by principal cells Gas1+ **b** Co-localization analysis for Gas1 and V-ATPase. **c** Pearson's coefficient correlation (PCC) for Gas1 and V-ATPase. In healthy and diabetic rats low values

of the PCC (>0.2) were observed indicating a very weak co-localization. It is important mentioned that even when all the PCC values are very low, we observed a discreet tendency to increase in the diabetic rats of seven, fourteen and twenty-one days. Gas1+ (red), V-ATPase+ (green) and DAPI+ (blue). Dotted white circles show magnifications of intercalated cells V-ATPase+ and principal cells Gas1+. Control (Ctrl); diabetes (dbt). Scale bars, 40 μ m and magnifications 22 μ m. Values are in mean \pm standard deviation (SD), * $p < 0.05$, ** $p < 0.01$, *** $p < 0.001$, **** $p < 0.0001$. All the experiments were performed in kidney sections. A representative experiment is shown (n=3)

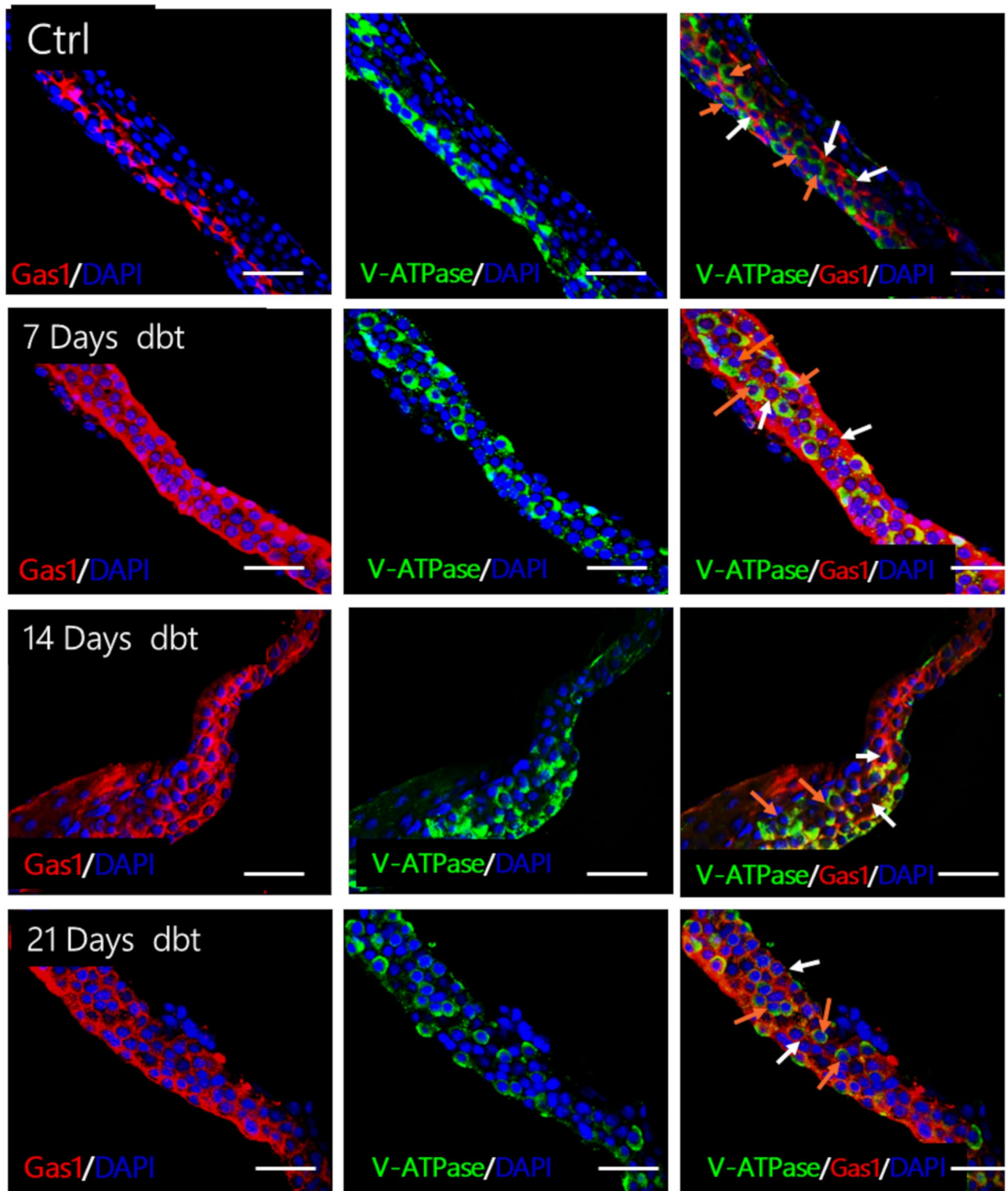


Fig. 5 Expression of Gas1 and V-ATPase on collecting ducts in the early stages of diabetes. **a** Immunofluorescence assays of Gas1 and V-ATPase on dissected collecting ducts from healthy and diabetic rats were performed. Gas1 and V-ATPase did not co-localize in the control rats. Most of the cells V-ATPase+ do not express Gas1 in diabetic rats

of 7, 14 and 21 days. Gas1+ (red), V-ATPase+ (green) and DAPI+ (blue). White arrows show Gas1+/V-ATPase- cells and orange arrows show Gas1-/V-ATPase+ cells. Control (Ctrl); diabetes (dbt). Scale bars, a=30 μ m and b=14 μ m. All the experiments were performed in isolated renal tubules. A representative experiment is shown (n=3)

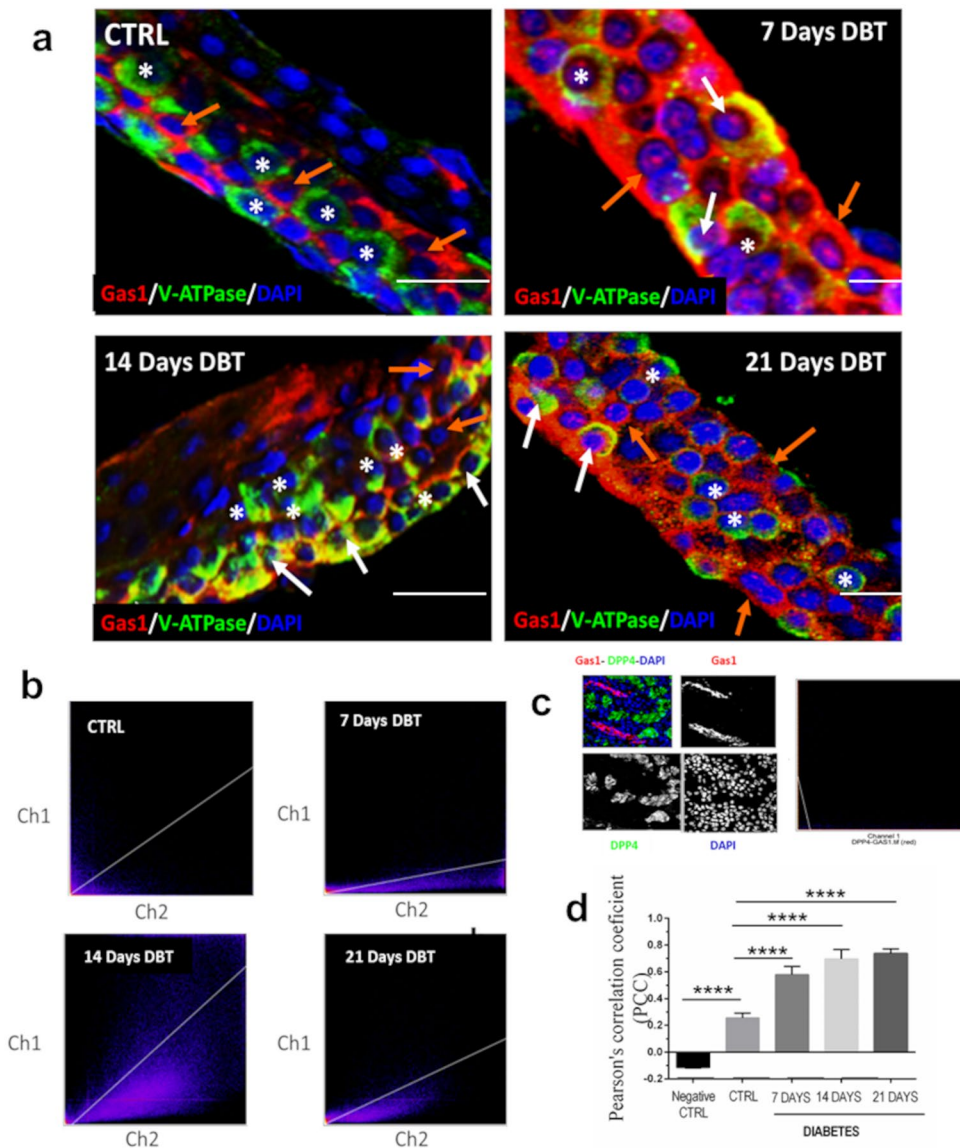


Fig. 6 A group of cells express Gas1 and V-ATPase in the early stages of diabetes. Previously we had found that principal cells express Gas1+ and intercalated cells do not, neither in control nor in diabetic rats. **a** Interestingly, few cells expressing both Gas1+ and V-ATPase+ were observed in diabetic rats of 7, 14 and 21 days. In the magnifications we can observe the co-localization of Gas1+ and V-ATPase+ (white arrows, yellow zones). **b** Co-localization analysis for Gas1 and V-ATPase. **c** Expression of Gas1 in the proximal tubule as negative control of co-localization. Immunofluorescence of Gas1 and the specific marker of proximal tubules dipeptidyl peptidase 4 (DPP4) was presented. **d** Pearson's coefficient correlation (PCC) for

Gas1 and V-ATPase. A low value of PCC was observed in healthy rats (0.25 ± 0.035) but in diabetic rats the PCC significantly increased (7 Days DBT, 0.58 ± 0.06 ; 14 Days DBT, 0.69 ± 0.070 ; 21 Days DBT, 0.73 ± 0.035). Gas1+ (red), V-ATPase+ (green) and DAPI+ (blue) in detail. White circles show magnifications of cells that express V-ATPase+ and Gas1+. White arrows show Gas1+/V-ATPase+ and Gas1+, orange arrows show Gas1+/V-ATPase- and white asterisks show Gas1-/V-ATPase+ cells. Control (Ctrl); diabetes (DBT). Scale bars, a=30 μm and b=13 μm. Values are in mean ± standard deviation (SD), * $p < 0.05$, ** $p < 0.01$, *** $p < 0.001$, **** $p < 0.0001$. All the experiments were performed in isolated renal tubules. A representative experiment is shown (n=3)

Gas1+ principal cells were observed compared with the controls. In contrast, at 14 days of diabetes a discrete but significant reduction in the number of AQP2+/Gas1+ principal cells were observed, and by 21 days of diabetes a significant increase in the number of cells was found. A tendency to increase the number of cells was observed at

7 and 21 days of diabetes (Fig. 7a). On the other hand, a significant reduction of V-ATPase+/Gas1- intercalated cells was observed in rats after 7, 14 and 21 days of diabetes compared with healthy rats (Fig. 7b). Diabetes favors the appearance of intermediated cells which express Gas1 and V-ATPase. In the quantification analysis 1–2 intermediates

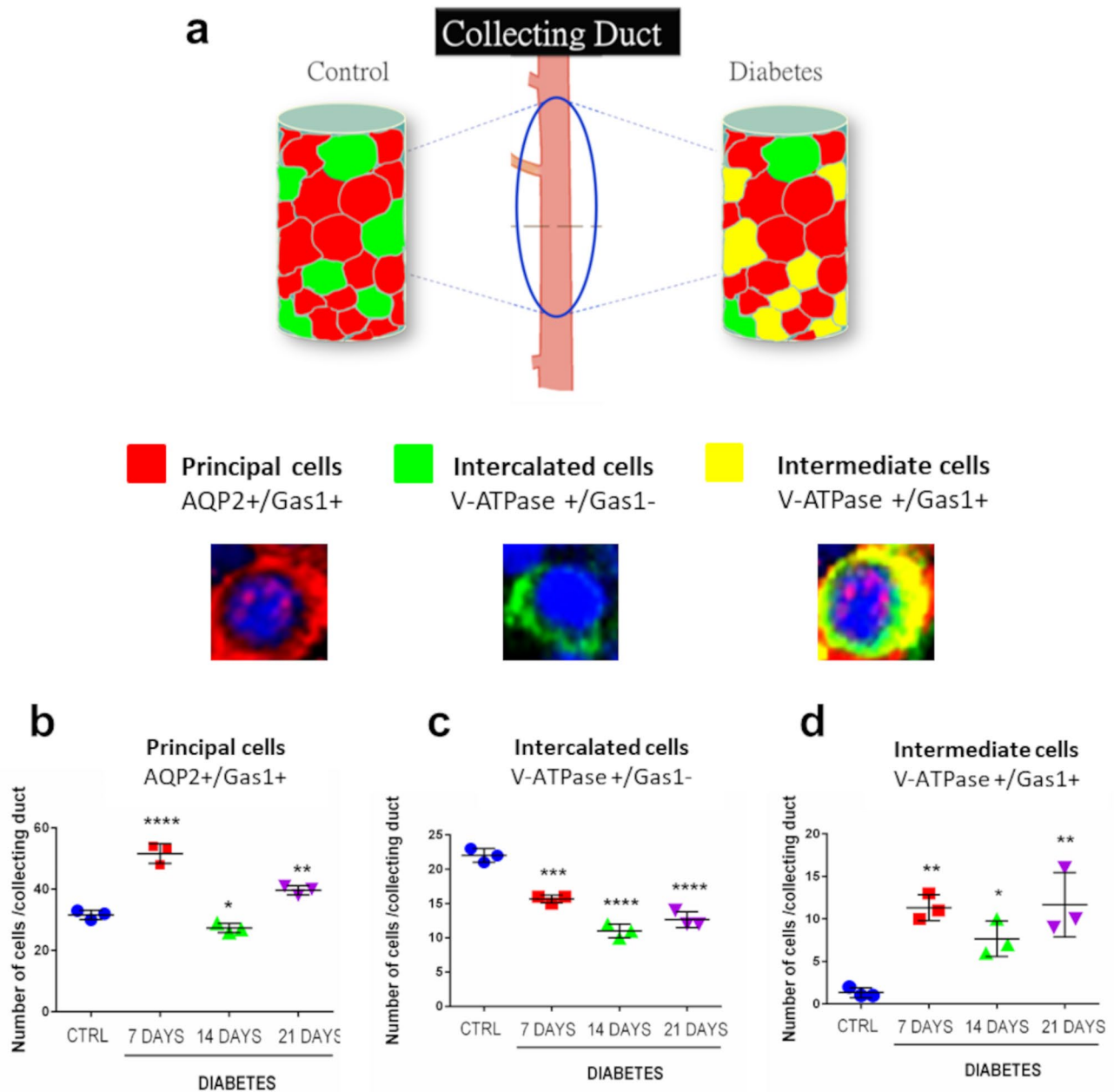


Fig. 7 Quantification of AQP2+/Gas1+ principal cells, V-ATPase+/Gas1- intercalated cells and cells that express both markers Gas1+/V-ATPase+ in the collecting ducts. **a** In healthy rats principal cells AQP2+/Gas1+ and intercalated cells V-ATPase+/Gas1- were observed. In diabetic rats, intercalated cells V-ATPase+/Gas1- were still detected but interestingly few cells which express V-ATPase+/Gas1+ were

observed and we identify them as intermediate cells. **b** Quantification of AQP2+/Gas1+ principal cells. **c** Quantification of V-ATPase+/Gas1- intercalated cells. **d** Quantification of V-ATPase+/Gas1+ intermediate cells. Gas1+ (red), V-ATPase+ (green) and DAPI+ (blue). All the experiments were performed in immunofluorescence images of isolated renal tubules. Values are means ± standard deviation (SD), * $p < 0.05$, ** $p < 0.01$, *** $p < 0.001$, **** $p < 0.0001$; $n = 3$

cells Gas1+/V-ATPase+ were detected in healthy rats but the number of cells Gas1+/V-ATPase+ significantly increased in diabetic rats (Fig. 7d) (Ctrl 0.66 ± 0.57 cells, 7 days DBT 11.3 ± 1.52 cells, 14 days DBT 7.6 ± 2.08 cells and 21 days DBT 11.6 ± 3.78 cells). The results

suggest that AQP2+ principal cells express Gas1 and the V-ATPase+ intercalated cells do not express Gas1. The early stages of diabetes induce a loss of intercalated cells, an initial increase of principal cells that changes with time and the increase of intermediate cells.

Principal cells express progenitor cells markers CD24 and CD133 in healthy and diabetic rats

Principal cells AQP2+ possess progenitor cell properties and can differentiate into intercalated cells in adult mouse kidney (Kim et al. 2016). In order to evaluate whether the principal cells AQP2+ which express Gas1 could also express progenitor cell markers like CD24 and CD133 in adult kidney under basal conditions or whether its expression is influenced by changes in the physiological microenvironment induced by the early stages of diabetes (hyperglycemia and inflammation) (Molina-Jijón et al. 2015; Sierra-Mondragon et al. 2018), we performed immunofluorescence assays in kidney sections to analyze the expression of AQP2, CD24 and CD133 (Fig. 8). Co-localization of AQP2 and CD24 was observed in both healthy and diabetic rats of 7, 14 and 21 days (Fig. 8a). Quantitative analysis of co-localization was determined. A moderate co-localization between Gas1 and CD24 was observed in both control and diabetic rats (Supplementary Fig. 5a-b). AQP2 and CD133 co-localized (yellow zones) in healthy and diabetic rats (Fig. 8b and Supplementary Fig. 5c-d). The results suggest that the AQP2+ principal cells express the progenitor cells markers CD24 and CD133 in both healthy and diabetic rats.

Expression of Gas1, AQP2, CD24 and V-ATPase in an enriched fraction of collecting ducts of healthy and diabetic rats

Enriched fractions of CD from renal medulla of healthy and diabetic rats were obtained, and since the tight junction protein claudin-4 (CLDN4) is highly expressed in the CD (Hou 2016), western blot analysis for CLDN4 was performed (Fig. 9a-b). The expression of CLDN4 was observed in control and diabetic rats indicating that the fractions of renal medulla of healthy and diabetic rats are enriched with CD. Moreover, the expression of Gas1 was detected in the glomerulus and brains of healthy and diabetic rats were used as positive control (Fig. 9c). The immunoblot of Gas1 in medullary fractions enriched with CD (Fig. 9d) reveals that Gas1 is expressed in healthy rats but during the first 7 days of diabetes its expression significantly increased compared with the control followed by a significant reduction in its expression at 14 days of diabetes. Later, Gas1 is overexpressed in comparison with healthy rats, in rats with 21 days of diabetes, suggesting that diabetes promotes the expression of Gas1. In the diabetic rats of 7 days, a slight increase in the expression of AQP2 was observed by western blot. In the diabetic rats of 14 days the expression of AQP2 was significantly decreased and by the 21 days of diabetes the

expression of AQP2 significantly increased compared to healthy rats. Western blot analysis shows expression of CD24 in healthy rats and an overexpression of CD24 in 7 days diabetic rats. At 14 days of diabetes a decrease in the expression of CD24 was observed and by 21 days of diabetes the expression of CD24 increased significantly compared with the healthy rats (Fig. 9e-f). Furthermore, a significant decrease of V-ATPase protein was found at the 7, 14 and 21 days of diabetes (Fig. 9g). The results indicated that Gas1 is expressed in an enriched fraction of CD of healthy and diabetic rats, confirming the previous results of immunofluorescence in kidney sections and isolated CD. A similar pattern of expression was observed in the immunoblots of the principal cells marker AQP2, Gas1 and CD24 compared with the intercalate cells marker V-ATPase. We observed the overexpression of Gas1, AQP2 and CD24 at 7 and 21 days of diabetes whereas a decrease in their expression was determined at 14 days of diabetes, pointing out that the three proteins have a similar response to diabetes. The results suggest that Gas1, AQP2 and CD24 are expressed in the same cell type in the CD and support the previous results obtained by immunofluorescence indicating that the AQP2+ principal cells express Gas1 as well as the progenitor cell markers CD24 and CD133. On the other hand, the decreased expression of V-ATPase is related with the decreased in the number of intercalated cells during diabetes, indicating that there is a loss of this cell type in the CD.

Distal tubules express Gas1 in healthy and diabetic rats

The expression of Gas1 was also explored in the distal tubules (DT) of healthy and diabetic rats. Immunofluorescence assays were performed in kidney sections to analyze the expression of Gas1 and calbindin (CALB), a specific marker of DT (Kobayashi et al. 2011; Lee et al. 2016) (Fig. 10). Gas1 and CALB have a similar pattern of expression in the DT in healthy and diabetic rats of 7, 14 and 21 days of diabetes, suggesting that Gas1 is expressed in the DT. To confirm the expression of Gas1; enriched fractions of DT from healthy and diabetic rats of 7, 14 and 21 days were obtained by Percoll density gradient (Fig. 11a-b). Expression of Gas1 was analyzed by western blot in the enriched fraction of DT of healthy and diabetic rats (Fig. 11d). Gas1 is expressed in healthy rats. In contrast at 7 days of diabetes the expression of Gas1 is slightly decreased but at both 14 and after 21 days of diabetes its expression is significantly increased. Also, the expression of Gas1 was analyzed by ELISA in the enriched fractions of DT. Expression of Gas1 was detected in healthy rats, in contrast in the first 7 days of diabetes a significant decrease of Gas1 was detected

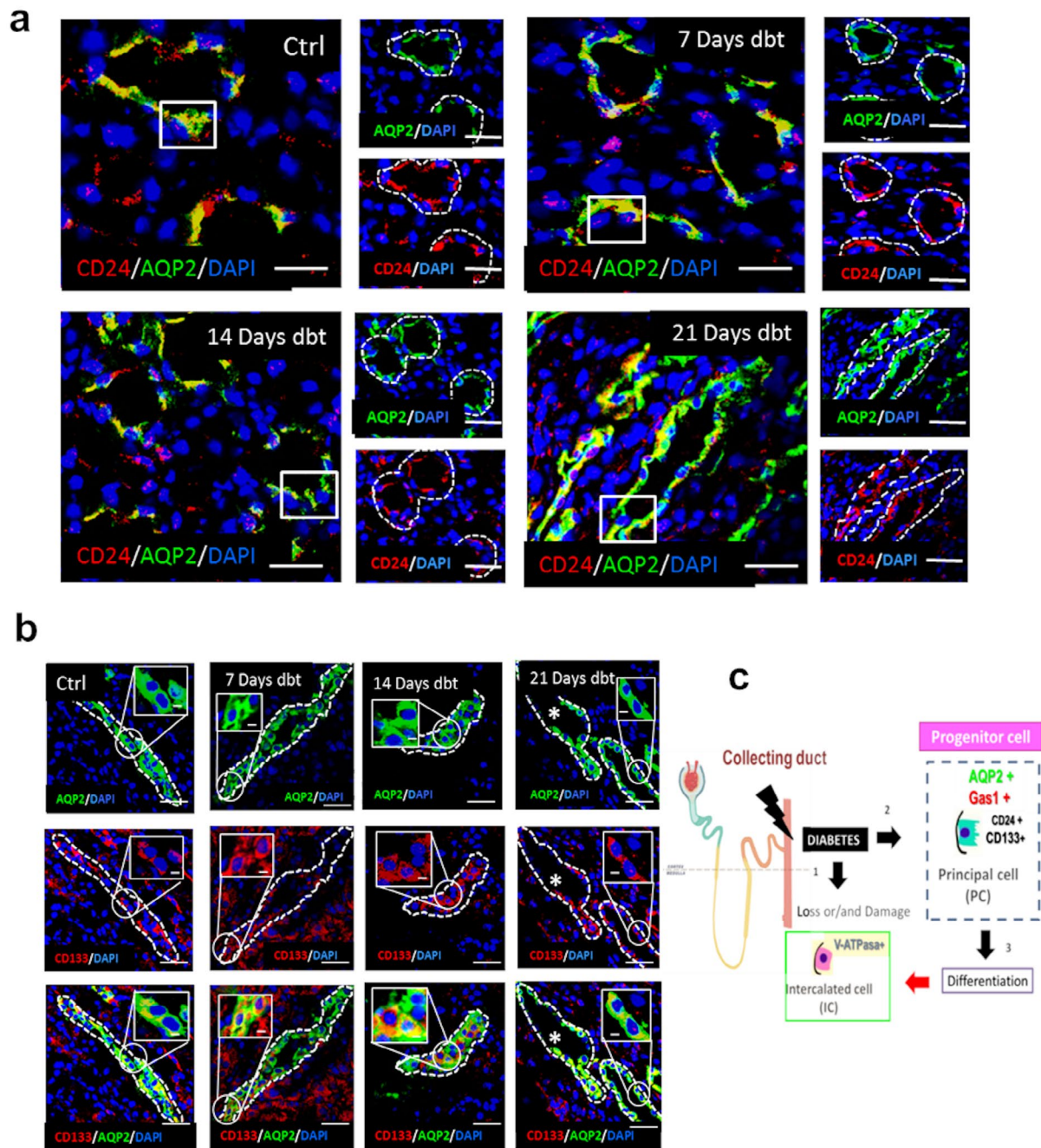


Fig. 8 The principal cells of the collecting duct express progenitor markers. **a** The expression of AQP2 and CD24 (progenitor cell marker) was analyzed by confocal microscopy in healthy and in the diabetic rats of seven, fourteen and twenty-one days. Collecting ducts were identified in the renal medulla. Expression of CD24+ was observed in the tubule structure in controls and in 7, 14 and 21 days of diabetes. CD24 and AQP2 co-localized in control and in diabetes (yellow zones). **b** Analysis of AQP2 and CD133 (progenitor marker). AQP2+ and CD133+ co-localized in healthy and diabetic rats of 7, 14 and 21 days. In the white boxes we can observe magnifications of the co-localization of AQP2 and CD133 cells (yellow zones). **c** 1 It is likely that in the early stages of diabetes a loss of V-ATPase+ intercalated

cells occurs. **2** We observed that in control as well as in diabetic conditions that the AQP2+ principal cells express progenitor cells markers (CD24+ and CD133+). **3** These results suggest that the AQP2+ principal cells might be progenitor cells which under certain conditions (hyperglycemia) may differentiate into intercalated cells. In a: CD24+ (red), AQP2+ (green) and DAPI+ (blue). White boxes indicated co-localization of AQP2+ /CD24+ cells. Scale bars, 40 μm. In b: CD133+ (red), AQP2+ (green) and DAPI+ (blue). White circles indicated magnifications of AQP2+/CD133+ cells. Dotted line delimits the tubular structure. Asterisks indicated tubular lumen. Scale bars, 40 μm and magnifications 27 μm. Control (Ctrl); diabetes (dbt). All the experiments were performed in kidney sections. A representative experiment is shown (n=3)

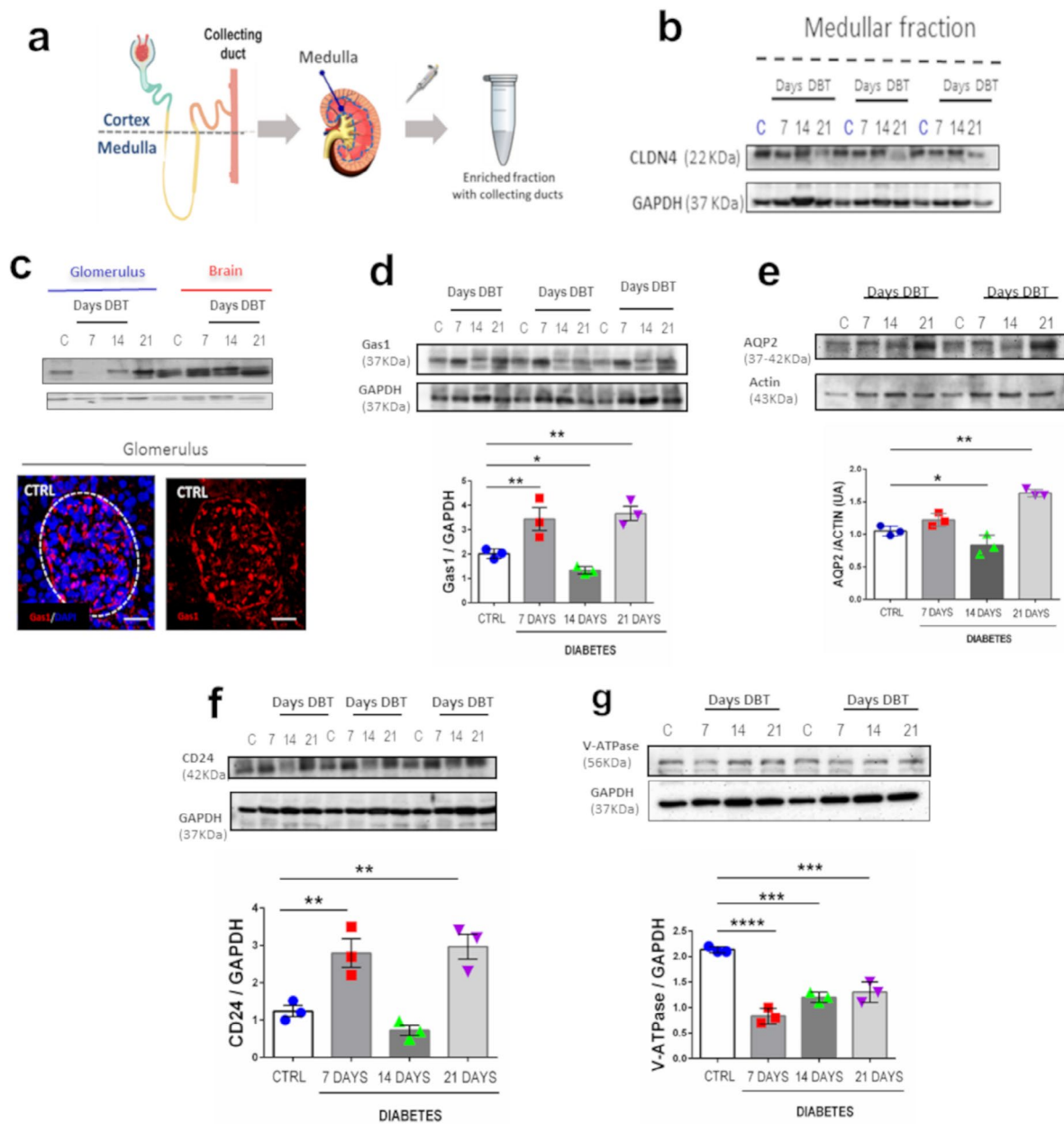
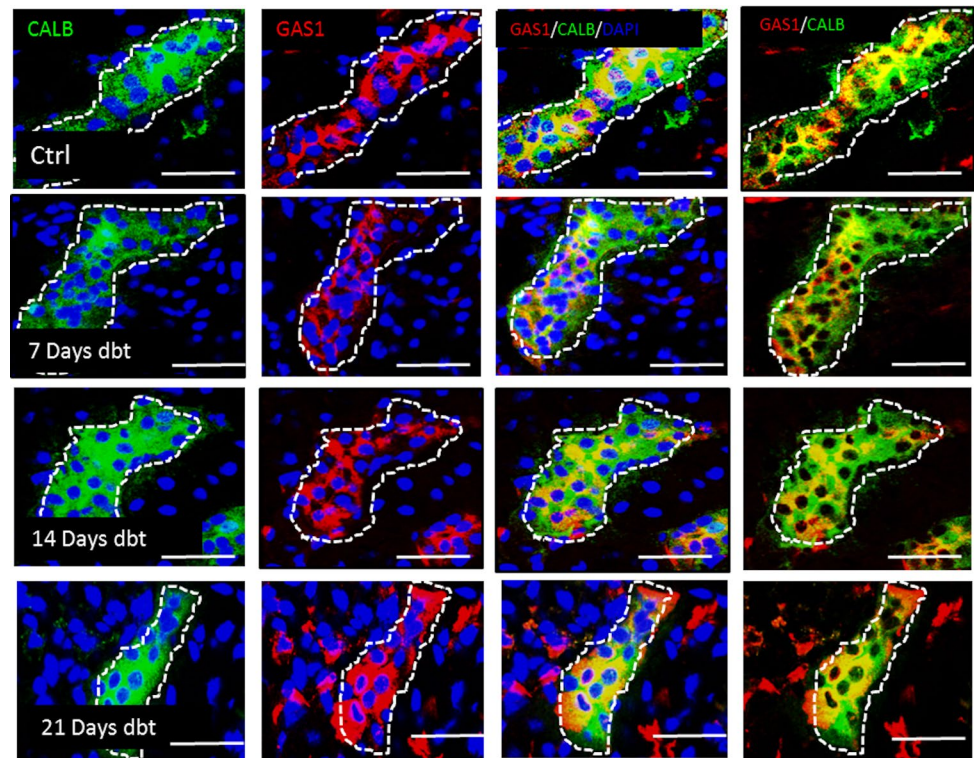


Fig. 9 The expression of Gas1, AQP2, CD24 and V-ATPase in an enriched fraction of collecting ducts. **a** An enriched fraction of collecting ducts from medulla was obtained. **b** Analysis by western blot of claudin-4 (CLDN4) in the fraction of renal medulla. The tight junction CLDN4 is highly expressed in the collecting ducts. We observed that CLDN4 is expressed in the control conditions and in 7, 14 and 21 days of diabetes, suggesting that the fraction of renal medulla is enriched by collecting ducts. **c** Positive control of Gas1 in kidney. We consider as a positive control the expression of Gas1 in the glomerular cells. We performed a western blot with an enriched fraction of glomerulus and brain from healthy rats and diabetic rats of 7, 14 and 21 days to support our results in the enriched fraction of collecting duct by western blot. We also present an immunofluorescence of Gas1 in a glomerulus to confirm the expression of Gas1 in glomerular cells and show the specificity of the antibody used to detect Gas1. The glomerulus has its typical spherical structure, the expression of Gas1 (in red) was observed in

the visceral zone (related with mesangial cells and podocytes) and in the periphery or Bowman's capsule (associated with parietal cells). **d** Analysis by western blot of Gas1. We observed that Gas1 is expressed in control conditions. In contrast, at 7 days of diabetes, the expression of Gas1 increased significantly compared with the control but in the 14 days of diabetes its expression decreased notably. At 21 days of diabetes the expression of Gas1 increased again to high levels. **e** Analysis by western blot of AQP2. **f** Analysis by western blot of CD24 **g** Analysis by western blot of V-ATPase. The expression of V-ATPase decreased significantly in the diabetic condition of 7, 14 and 21 days compared with the control. Gas1+ (red) and DAPI+ (blue). Dotted line delimits the glomerulus. Scale bar 50 μ m. Densitometric analysis of western blot is shown. Data for control and diabetic groups are expressed as relative density from six rats/group normalized to actin or GAPDH as loading control. Values are means \pm standard deviation (SD), * $p < 0.05$, ** $p < 0.01$, *** $p < 0.001$, **** $p < 0.0001$

Fig. 10 Expression of Gas1 in the distal tubules. An immunofluorescence analysis of Gas1 and calbindin (CALB) was performed. In the tubular structure Gas1 and CALB have a similar pattern of expression in both controls and at the 7, 14 and 21 days of diabetes. This result suggest that Gas1 could be expressed in the distal tubules. Gas1+ (red), CLAB+ (green) and DAPI+ (blue). White arrows indicate magnification of Gas1+ /CALB+ cells. Dotted line delimits the tubular structure. Control (Ctrl); diabetes (dbt). Scale bars, 30 μ m. All the experiments were performed in kidney sections. A representative experiment is shown (n=3)



followed by a significant increase at 21 days of diabetes, confirming the results obtained by western blot. The results indicate that distal tubule cells express Gas1 in healthy and diabetic rats.

In the CD the expression of the progenitor cell markers CD24 and CD133 was observed in AQP2+ principal cells. Thus, we decided to study whether distal tubule cells express CD24 and Gas1. Immunofluorescence assays of Gas1 and CD24 were performed in the DT in kidney sections of both healthy and diabetic rats (Fig. 11f). Quantitative colocalization analysis shows a moderate co-localization of Gas1 and CD24 in healthy and diabetic rats of 7, 14 and 21 days (Supplementary Fig. 6). The expression of CD24 was also analyzed by western blot in the enriched fraction of DT of healthy and diabetic rats (Fig. 11e). Expression of CD24 was observed in healthy rats. In contrast in the diabetic rats of 7 days the expression of CD24 significantly decreased compared with healthy rats. In rats of 14 and 21 days of diabetes, Gas1 is overexpressed. Gas1 and CD24 have a similar pattern of expression as assessed by western blot, the expression of both proteins decreases at 7 days of diabetes and significantly increase by the 14 and 21 days of diabetes. The results suggest that the DT cells express Gas1 and also the progenitor cell marker CD24 in healthy and diabetic rats. Furthermore, diabetes promotes the increase of Gas1 and CD24 expression in the DT at 14 and 21 days of diabetes.

Discussion

The expression of Gas1 was examined in the CD ducts of healthy rats and during the early stages of diabetes. The main findings of this study are: (1) the principal cells of the CD specifically express Gas1 in healthy and diabetic rats; (2) the principal cells express the progenitor cell markers CD24 and CD133 in healthy and diabetic rats; (3) diabetes promotes the presence of intermediate cells that express both principal and intercalated cell markers (Gas1+/V-ATPase+) in the CD; (4) diabetes promotes the decrease of V-ATPase+ intercalated cells; and (5) that the distal tubule cells also express Gas1. This is the first study describing the expression of Gas1 in the collecting ducts and distal tubules during the early stages of diabetes.

The results show that Gas1 is expressed in the CD and that its expression is mostly in the principal cells (AQP2+/Gas1+), suggesting that Gas1 is a specific marker of principal cells. Collecting ducts and glomerular cells come from distinct embryonic precursors, thus they have a different cell lineage. Glomerular cells are derived from the progenitor cells of the metanephric mesenchyme and, the CD from the ureteral bud (McMahon 2016; Chen et al. 2017). Gas1 is expressed during nephrogenesis in the cap mesenchyme but not in the ureteric bud (Kann et al. 2015). Considering this, it was assumed that only glomerular cells would express Gas1. It is likely that the expression of Gas1 occurs postnatally in the CD. A recent study showed that the

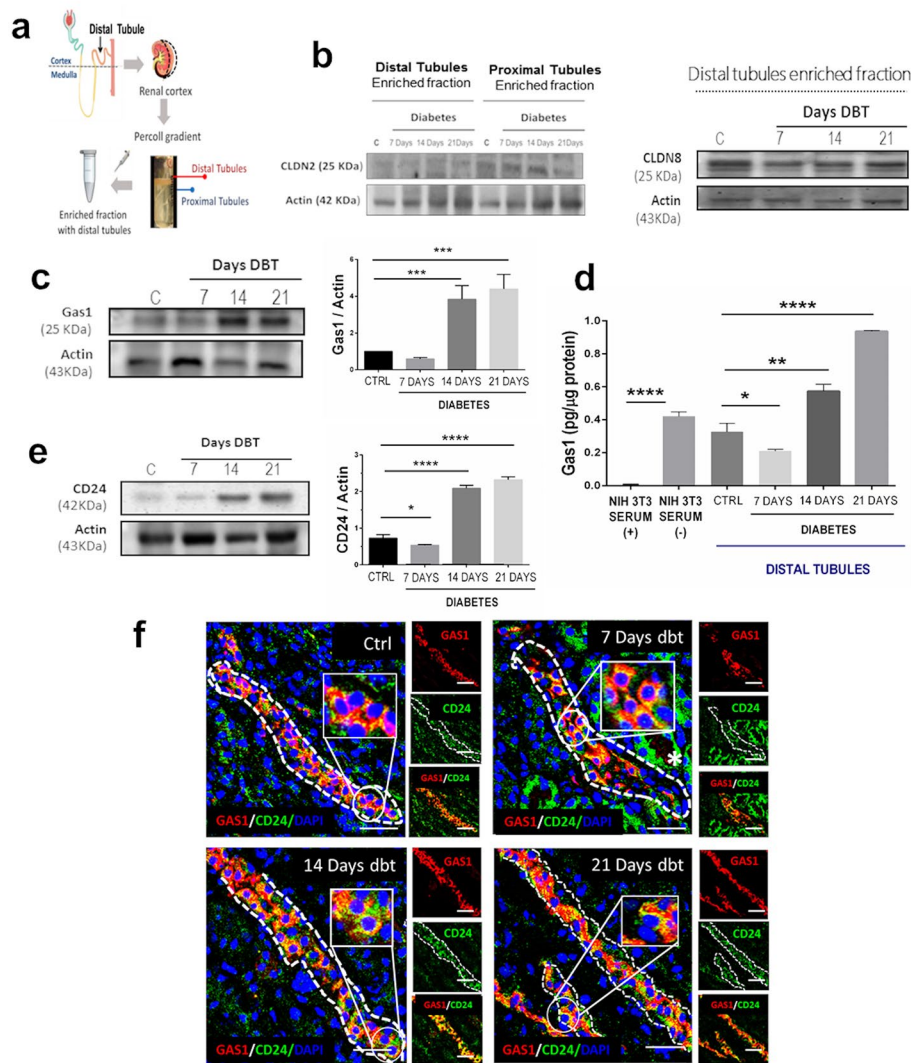


Fig. 11 Expression of Gas1 in an enriched fraction of distal tubules. **a** Schematic representation. A Percoll gradient was performed from renal cortex to obtain an enriched fraction of distal tubules. **b** Western blot analysis of the expression of claudin-2 (CLDN2) in the isolated fraction of distal tubules (DT) and proximal tubules (PT) to determine the purity of our sample. CLDN2 is a tight junction protein abundantly expressed in the proximal tubules. We observed that in the isolated fraction of DT the expression of CLDN2 is absent. In contrast, in the fraction of PT we observed expression of CLDN2. Also, the expression of CLDN8 (tight junction protein expressed in DT) was analyzed. We observed that in control and in the diabetic conditions CLDN8 is consistently expressed in the fraction of distal tubules, indicating the presence and enrichment of distal tubules in the fraction isolated by Percoll gradient. **c** Analysis by ELISA of Gas1 in the enriched fraction of distal tubules. Gas1 is expressed in controls but at 7 days of diabetes the expression of Gas1 decreased in comparison with controls. In contrast, at the 14 and 21 days of diabetes the expression of Gas1 significantly increased. We used as positive control NIH 3T3

cells with serum starvation. **d** Analyzed by western blot of Gas1 in the enriched fraction of distal tubules. **e** Expression of CD24 in distal tubules by western blot. CD24 is expressed in the controls but by 7 days of diabetes the expression of CD24 decreased significantly and at 14 and 21 day of diabetes its expression significantly increased. **f** Expression of Gas1 and CD24 in the distal tubules. An immunofluorescence analysis of Gas1 and CD24 was performed. Gas1 and CD24 co-localized in healthy and diabetic rats of 7, 14 and 21 days. In the magnifications, the co-localization of Gas1 and CD24 is observed. Densitometric analysis of western blot is shown. Data for control and diabetic groups are expressed as relative density from six rats/group normalized to actin as loading control. Values are means \pm standard deviation (SD), * $p < 0.05$, ** $p < 0.01$, *** $p < 0.001$, **** $p < 0.0001$. In the immunofluorescence: Gas1+ (red), CD24+ (green) and DAPI+ (blue). White circles indicate magnification of Gas1+/CD24+ cells. Dotted line delimits the tubular structure. Asterisks indicated other tubular structures like proximal tubules. Control (Ctrl); diabetes (dbt). Scale bars, 30 μ m and magnifications 14 μ m A representative experiment is shown (n = 3)

transcriptional factor Elf5 is an early maker of the principal cell lineage that contributes to the expression of principal cell specific genes, it is then possible that this transcription

factor has an important role in the specific expression of Gas1 in the principal cells of mature CD (Grassmeyer et al. 2017).

The enriched fractions of CD showed that Gas1 is expressed in healthy rats. In contrast, in the 7 and 21 days diabetic rats Gas1 is overexpressed. Until now the expression of Gas1 in CD was unknown and thus the alterations of its expression induced by metabolic alterations such as diabetes. In medullary CD high NaCl levels increase the expression of PAX2, suggesting that PAX2 is an osmo-regulated protein (Cai et al. 2004). Under diabetic conditions, the activity of the renin–angiotensin–aldosterone system (RAAS) is increased, resulting in overproduction of vasopressin and aldosterone (ALD), leading to an increase in the osmolality of renal medullary interstitial fluid with high concentrations of NaCl and urea (Rincon-Choles et al. 2003; Siragy et al. 2003; Hollenberg et al. 2004). Previous results demonstrated that in diabetic rats of 21 days treated with STZ, the serum levels of ALD and osmolality were increased (Molina-Jijón et al. 2017). Thus, overexpression of Gas1 in the medullary CD could be associated with the increase in the osmolality and the osmotic tolerance of cells. The high osmolality during early stages of diabetes may be a consequence of the high blood glucose concentration or the activation of the RAAS system.

The CD possesses a heterogeneous cell morphology composed of intercalated cells specifically expressing V-ATPase and AE-1; and principal cells which express AQP2, AQP4, and as we now show Gas1 (Pearce et al. 2015; Roy et al. 2015). Changes in the cell morphology of the CD were found during the early stages of diabetes in this study. In STZ-diabetic rats, the number of principal cells AQP2+/Gas1+ increases significantly at 7 and 21 days of diabetes. In contrast, the number of V-ATPase+/Gas1-intercalated cells significantly decreased in all diabetic rats. Interestingly, it was also observed that diabetes induces the appearance of Gas1+/V-ATPase+ cells in the CD. Previous studies have described the presence of cells expressing both principal cell and intercalated cell markers, identifying them as intermediate cells. Rats with potassium depletion (DK), showed an increase of V-ATPase+/AQP4+ intermediate cells at 7 and 14 days of hypokalemia (Iervolino et al. 2020). Also in a lithium-induced nephrogenic diabetes *insipidus* model, some AE-1+/AQP2+ and V-ATPase+/AQP4+ intermediate cells were identified in adult rat CD (Trepiccione et al. 2013). These findings are in agreement with our results showing a significant increase of V-ATPase+/GAS1+ intermediate cells in diabetic rats of 7, 14 and 21 days. These results are the first changes reported in the cellular morphology of the CD induced by diabetes in STZ-treated rats.

Hoxb7-GFP+ cells derived from adult mouse CD display mesenchymal stem cells (MSCs) properties like clonogenicity, panmesodermal potential and long-term expansion. These MSC-like cells were positive for the renal progenitor/stem cell marker CD24 and they presented a

phenotype of AQP2+ principal cells, suggesting that principal cells are progenitor/ stem cells (Li et al. 2014). Another study showed that AQP2-EYFP+ principal cells acquire a phenotype of AQP2-/V-ATPase+ intercalated cells after K+ depletion, suggesting that AQP2+ principal cells can differentiate to intercalated cells in adult mouse kidney (Kim et al. 2016). In addition, in mice lacking histone H3 K79 methyltransferase Dot11 (Dot11^{AC} mice), principal cells can differentiate into intercalated cells and this process is enhanced by Dot11 deletion, demonstrating that intercalated cells are derived from AQP2+ principal cells suggesting its potential role as progenitor cells (Wu et al. 2013). Our results show that AQP2+ principal cells specifically express Gas1 and also progenitor cell markers (CD24 and CD133); the intercalated cells do not express Gas1 in neither healthy nor diabetic rats and diabetes promotes the presence of Gas1+/V-ATPase+ intermediate cells and also the decrease of intercalated cells. It is possible that due to the loss of V-ATPase+/Gas- intercalated cells in the early stages of diabetes, the AQP2+ principal cells that express Gas1 and also CD133 and CD24 might act as a progenitor cells and differentiate into intercalated cells to restore the diminished population of intercalated cells. The Gas1+/V-ATPase+ intermediate cells that were observed in the diabetic condition could be an intermediate step in the differentiation process of the principal cells (AQP2+/Gas1+) to intercalated cells (V-ATPase+/Gas1-) and they might be cells that are acquiring the specific markers of intercalated cells in diabetes. The results of this study provide evidence that AQP2+ principal cells express progenitor cell markers and suggest that during the early stages of diabetes principal cells differentiate to intercalated cells as a mechanism of regeneration/protection against hyperglycemia (Fig. 8c).

Until now there were no reports of the function of Gas1 in the CD. Our results indicate that the principal cells express Gas1 as well as progenitor cell markers (CD24+, CD133+). We suggest that Gas1 participates in the differentiation and maintenance of the principal cells in the CD as previously described during the early stages of nephrogenesis, or in the progenitor parietal cells of Bowman's capsule as it has been proposed during the development of the cortex and of the dentate gyrus of the mouse brain (Estudillo et al. 2016; Luna-Antonio et al. 2017). Previous results described the interaction of Gas1 with Delta-like protein 1 (Dlk1) suggesting that the interaction between Dlk1 and GAS1 could be of importance in cell differentiation processes (Baladrón et al. 2005). In the CD, Notch signaling can promote the differentiation of mature principal cells to intercalated cells (Mukherjee et al. 2019). It is likely that Gas1 has a role in the differentiation process of principal cells through the interaction with the components of the notch pathway. On the other hand, a role for Gas1 in cell viability, through the up-regulation

of the nuclear-localized protein-kinase Dyrk1B in mouse embryo fibroblast cells, has been reported (Pérez-Sánchez et al. 2018). Dyrk1B has been found in nuclear fractions of CD cells but its function remains unknown (Bolger et al. 2012). We suggest that the increase in the expression of Gas1 in the principal cells also might also be associated with a protective mechanism in the early stages of diabetes.

In addition, calbindin and Gas1 co-localized in both healthy and diabetic rats, suggesting that distal tubule cells express Gas1. The expression of Gas1 decreased at 7 days of diabetes but by 14 and 21 days of diabetes the expression of Gas1 significantly increased compared to healthy rats, as determined both by western blot and ELISA. An observation that caught our attention was the pattern of the expression of Gas1 in this segment of the nephron. The expression of Gas1 in the distal tubules in 7, 14 and 21 days of diabetes was different compared with the CD. The DT and CD are nephron segments derived from different embryonic precursors and, as expected, they are renal structures with morphological and functional differences (Costantini and Shakya 2006). The DT are derived from progenitor SIX2+ cells from the metanephric mesenchyme (Kobayashi et al. 2008). Previous studies have described the role of Gas1 in the maintenance of progenitor SIX2+ cells during nephrogenesis. It is possible that DT cells derived from precursor Gas1+/SIX2+ cells might maintain certain markers (Gas1+) in their differentiated state (Kann et al. 2015). Gas1 is a pleiotropic protein, thus we suggest that in the diverse nephron segments, Gas1 expression and function might be different. On the other hand, we noticed the co-expression of Gas1 with the progenitor cell marker CD24. This result is interesting since in the CD Gas1 is expressed in principal cells which also express progenitor cell markers (CD24/CD133) and previous results described the expression of Gas1 in progenitor parietal cells (NCAM+) in Bowman's capsule (Luna-Antonio et al. 2017). This provides strong evidence that Gas1 might have a novel function involved in the maintenance of progenitor cells in mature kidneys, and possibly in the differentiation process as an initial renal response to diabetes.

This study describes the expression of Gas1 in the collecting and distal tubules in healthy and diabetic rats. The results show the specific expression of Gas1 in the AQP2+ principal cells of collecting ducts and describe the expression of progenitor cells markers (CD24 and CD133) in these cells in both healthy and diabetic rats treated with STZ. Furthermore, we described the diabetes-induced changes in the cell morphology of the collecting duct: a notable decrease of intercalated cells (V-ATPase+/Gas1-) and the increase of intermediate cells (Gas1+/V-ATPase+). The results identify Gas1 as a novel marker of principal cells, suggest that diabetes promotes the expression of Gas1 and finally support

the capacity of AQP2+ principal cells to differentiate into intercalated cells. Future research addressing the function of Gas1 in the principal cells and its role in the renal response to diabetes will be necessary.

Supplementary Information The online version contains supplementary material available at <https://doi.org/10.1007/s10735-022-10104-7>.

Funding The research leading to these results received funding from Consejo Nacional de Ciencia y Tecnología (CONACyT) to Brenda I. Luna-Antonio under Grant Agreement 514,913. Partial financial support was received from CONACyT Fronteras de la Ciencia Grant Agreement 1563 to JS.

Declarations

Conflicts of interest/Competing interest The authors have no competing interests to declare that are relevant to the research, authorship, and/or publication of this article.

References

- Allen BL, Tenzen T, McMahon AP (2007) The Hedgehog-binding proteins Gas1 and Cdo cooperate to positively regulate Shh signaling during mouse development. *Genes Dev* 21:1244–1257. <https://doi.org/10.1101/gad.1543607>
- Andersen H, Friis UG, Hansen PBL et al (2015) Diabetic nephropathy is associated with increased urine excretion of proteases plasmin, prostatic and urokinase and activation of amiloride-sensitive current in collecting duct cells. *Nephrol Dial Transplant* 30:781–789. <https://doi.org/10.1093/ndt/gfu402>
- Arreola-Mendoza L, Reyes JL, Melendez E et al (2006) Alpha-tocopherol protects against the renal damage caused by potassium dichromate. *Toxicology* 218:237–246. <https://doi.org/10.1016/j.tox.2005.11.010>
- Ayala-Sarmiento AE, Estudillo E, Pérez-Sánchez G et al (2016) GAS1 is present in the cerebrospinal fluid and is expressed in the choroid plexus of the adult rat. *Histochem Cell Biol* 146:325–336. <https://doi.org/10.1007/s00418-016-1449-0>
- Baladrón V, Ruiz-Hidalgo MJ, Nueda ML et al (2005) Dlk acts as a negative regulator of Notch1 activation through interactions with specific EGF-like repeats. *Exp Cell Res* 303:343–359. <https://doi.org/10.1016/j.yexcr.2004.10.001>
- Bolger SJ, Hurtado PAG, Hoffert JD et al (2012) Quantitative phosphoproteomics in nuclei of vasopressin-sensitive renal collecting duct cells. *Am J Physiol Physiol* 303:C1006–C1020. <https://doi.org/10.1152/ajpcell.00260.2012>
- Brown D, Paunescu TG, Breton S, Marshansky V (2009) Regulation of the V-ATPase in kidney epithelial cells: Dual role in acid-base homeostasis and vesicle trafficking. *J Exp Biol* 212:1762–1772
- Cabrera JR, Sanchez-Pulido L, Rojas AM et al (2006) Gas1 is related to the glial cell-derived neurotrophic factor family receptors α and regulates Ret signaling. *J Biol Chem* 281:14330–14339. <https://doi.org/10.1074/jbc.M509572200>
- Cai Q, Dmitrieva NI, Ferraris JD et al (2004) Pax2 expression occurs in renal medullary epithelial cells in vivo and in cell culture, is osmoregulated, and promotes osmotic tolerance. *Proc Natl Acad Sci* 102:503–508. <https://doi.org/10.1073/pnas.0408840102>
- Campbell RC, Ruggenenti P, Remuzzi G (2003) Proteinuria in diabetic nephropathy: Treatment and evolution. *Curr Diab Rep* 3:497–504

- Chen L, Higgins PJ, Zhang W (2017) Kidney Development and Disease. *Costantini F, Shakya R (2006) GDNF/Ret signaling and the development of the kidney. BioEssays 28:117–127. <https://doi.org/10.1002/bies.20357>*
- Del Sal G, Collavin L, Ruaro ME et al (1994) Structure, function, and chromosome mapping of the growth-suppressing human homologue of the murine *gas1* gene. *Proc Natl Acad Sci U S A 91:1848–1852. <https://doi.org/10.1073/pnas.91.5.1848>*
- Del Sal G, Ruaro ME, Philipson L, Schneider C (1992) The growth arrest-specific gene, *gas1*, is involved in growth suppression. *Cell 70:595–607. [https://doi.org/10.1016/0092-8674\(92\)90429-G](https://doi.org/10.1016/0092-8674(92)90429-G)*
- Dominguez-Monzon G (2011) Molecular Mechanisms of Action of Gas1 and its Possible Therapeutic Applications. *Curr Signal Transduct Ther 6:106–112*
- Dominguez-Monzon G, Benitez JA, Vergara P et al (2009) Gas1 inhibits cell proliferation and induces apoptosis of human primary gliomas in the absence of Shh. *Int J Dev Neurosci 27:305–313. [https://doi.org/S0736-5748\(09\)00041-0](https://doi.org/S0736-5748(09)00041-0) [pii]10.1016/j.ijdevneu.2009.03.009*
- Dunn KW, Kamocka MM, McDonald JH (2011) A practical guide to evaluating co-localization in biological microscopy. *Am. J. Physiol. - Cell Physiol. 300*
- Estudillo E, Zavala P, Pérez-Sánchez G et al (2016) Gas1 is present in germinal niches of developing dentate gyrus and cortex. *Cell Tissue Res 364:369–384. <https://doi.org/10.1007/s00441-015-2338-x>*
- Girardi ACC, Knaufl F, Demuth HU, Aronson PS (2004) Role of dipeptidyl peptidase IV in regulating activity of Na⁺/H⁺ exchanger isoform NHE3 in proximal tubule cells. *Am J Physiol - Cell Physiol 287. <https://doi.org/10.1152/ajpcell.00186.2004>*
- Gonzalez-Mariscal L, Namorado MC, Martin D et al (2000) Tight junction proteins ZO-1, ZO-2, and occludin along isolated renal tubules. *Kidney Int 57:2386–2402. <https://doi.org/10.1046/j.1523-1755.2000.00098.x>*
- Grassmeyer J, Mukherjee M, deRiso J et al (2017) Elf5 is a principal cell lineage specific transcription factor in the kidney that contributes to Aqp2 and Avpr2 gene expression. *Dev Biol 424:77–89. <https://doi.org/10.1016/j.ydbio.2017.02.007>*
- Habib SL (2013) Alterations in tubular epithelial cells in diabetic nephropathy. *J Nephrol 26:865–869. <https://doi.org/10.5301/jn.5000287>*
- Hervey GR (1953) Determination of Creatinine by the Jaffe Reaction. *Nature 171:1125. <https://doi.org/10.1038/1711125a0>*
- Hollenberg NK, Stevanovic R, Agarwal A et al (2004) Plasma aldosterone concentration in the patient with diabetes mellitus: Rapid communication. *Kidney Int 65:1435–1439. <https://doi.org/10.1111/j.1523-1755.2004.00524.x>*
- Holthofer H, Schulte BA, Pasternack G et al (1987) Three distinct cell populations in rat kidney collecting duct. *Am J Physiol - Cell Physiol. <https://doi.org/10.1152/ajpcell.1987.253.2.c323>. 253:*
- Hou J (2016) Paracellular transport in the collecting duct. *Curr Opin Nephrol Hypertens 25:424–428*
- Iervolino A, Prosperi F, De La Motte LR et al (2020) Potassium depletion induces cellular conversion in the outer medullary collecting duct altering Notch signaling pathway. *Sci Rep 10. <https://doi.org/10.1038/s41598-020-61882-7>*
- Jerums G, Premaratne E, Panagiotopoulos S, MacIsaac RJ (2010) The clinical significance of hyperfiltration in diabetes. *Diabetologia 53:2093–2104*
- Jung HJ, Kwon TH (2016) Molecular mechanisms regulating aquaporin-2 in kidney collecting duct. *Am J Physiol - Ren Physiol 311:F1318–F1328*
- Kann M, Bae E, Lenz MO et al (2015) WT1 targets Gas1 to maintain nephron progenitor cells by modulating FGF signals. *Development 142:1254–1266. <https://doi.org/10.1242/dev.119735>*
- Kim WY, Nam SA, Choi A et al (2016) Aquaporin 2-labeled cells differentiate to intercalated cells in response to potassium depletion. *Histochem Cell Biol 145:17–24. <https://doi.org/10.1007/s00418-015-1372-9>*
- Kobayashi A, Valerius MT, Mugford JW et al (2008) Six2 Defines and Regulates a Multipotent Self-Renewing Nephron Progenitor Population throughout Mammalian Kidney Development. *Cell Stem Cell 3:169–181. <https://doi.org/10.1016/j.stem.2008.05.020>*
- Kobayashi M, Yasuoka Y, Sato Y et al (2011) Upregulation of calbindin D28k in the late distal tubules in the potassium-loaded adrenalectomized mouse kidney. *Clin Exp Nephrol 15:355–362. <https://doi.org/10.1007/s10157-011-0414-4>*
- Lee C, Te, Ng HY, Lee YT et al (2016) The role of calbindin-D28k on renal calcium and magnesium handling during treatment with loop and thiazide diuretics. *Am J Physiol - Ren Physiol 310:F230–F236. <https://doi.org/10.1152/ajprenal.00057.2015>*
- Li J, Ariunbold U, Suhaimi N et al (2014) Collecting Duct-Derived Cells Display Mesenchymal Stem Cell Properties and Retain Selective In Vitro and In Vivo Epithelial Capacity. *J Am Soc Nephrol 26:81–94. <https://doi.org/10.1681/asn.2013050517>*
- Li Q, Qin Y, Wei P et al (2016) Gas1 inhibits metastatic and metabolic phenotypes in colorectal Carcinoma. *Mol Cancer Res 14:830–840. <https://doi.org/10.1158/1541-7786.MCR-16-0032>*
- Lim AKH (2014) Diabetic nephropathy – Complications and treatment. *Int J Nephrol Renovasc Dis 7:361–381. <https://doi.org/10.2147/IJNRD.S40172>*
- López-Ornelas A, Mejía-Castillo T, Vergara P, Segovia J (2011) Lentiviral transfer of an inducible transgene expressing a soluble form of Gas1 causes glioma cell arrest, apoptosis and inhibits tumor growth. *Cancer Gene Ther 18:87–99. <https://doi.org/10.1038/cgt.2010.54>*
- López-Ornelas A, Vergara P, Segovia J (2014) Neural stem cells producing an inducible and soluble form of Gas1 target and inhibit intracranial glioma growth. *Cytotherapy 16:1011–1023. <https://doi.org/10.1016/j.jcyt.2013.12.004>*
- López-Ramírez MA, Domínguez-Monzón G, Vergara P, Segovia J (2008) Gas1 reduces Ret tyrosine 1062 phosphorylation and alters GDNF-mediated intracellular signaling. *Int J Dev Neurosci 26:497–503. <https://doi.org/10.1016/j.ijdevneu.2008.02.006>*
- Luna-Antonio BI, Rodríguez-Muñoz R, Namorado-Tonix C et al (2017) Gas1 expression in parietal cells of Bowman's capsule in experimental diabetic nephropathy. *Histochem Cell Biol 148:33–47. <https://doi.org/10.1007/s00418-017-1550-z>*
- Ma Y, Qin H, Cui Y (2013) MiR-34a targets GAS1 to promote cell proliferation and inhibit apoptosis in papillary thyroid carcinoma via PI3K/Akt/Bad pathway. *Biochem Biophys Res Commun 441:958–963. <https://doi.org/10.1016/j.bbrc.2013.11.010>*
- Madsen KM, Tisher CC (1986) Structural-functional relationships along the distal nephron. *Am. J. Physiol. - Ren. Fluid Electrolyte Physiol. 250*
- Martinelli DC, Fan C-M (2007) The role of Gas1 in embryonic development and its implications for human disease. *Cell Cycle 6:2650–2655*
- McMahon AP (2016) Development of the Mammalian Kidney, 1st edn. Elsevier Inc
- Meeme A, Kasozi H (2009) Effect of glycaemic control on glomerular filtration rate in diabetes mellitus patients. *Afr Health Sci 9. <https://doi.org/10.4314/ahs.v9i2.47808>. Suppl 1*
- Mellström B, Ceña V, Lamas M et al (2002) Gas1 is induced during and participates in excitotoxic neuronal death. *Mol Cell Neurosci 19:417–429. <https://doi.org/10.1006/mcne.2001.1092>*
- Molina-Jijón E, Rodríguez-Muñoz R, del Namorado M et al (2015) All-trans retinoic acid prevents oxidative stress-induced loss of renal tight junction proteins in type-1 diabetic model. *J Nutr Biochem 26:441–454. <https://doi.org/10.1016/j.jnutbio.2014.11.018>*

- Molina-Jijón E, Rodríguez-Muñoz R, González-Ramírez R et al (2017) Aldosterone signaling regulates the over-expression of claudin-4 and -8 at the distal nephron from type 1 diabetic rats. *PLoS ONE* 12:e0177362. <https://doi.org/10.1371/journal.pone.0177362>
- Molina-Jijón E, Rodríguez-Muñoz R, Namorado MDC et al (2014) Oxidative stress induces claudin-2 nitration in experimental type 1 diabetic nephropathy. *Free Radic Biol Med* 72 C:162–175. <https://doi.org/10.1016/j.freeradbiomed.2014.03.040>
- Moser B, Hochreiter B, Herbst R, Schmid JA (2017) Fluorescence colocalization microscopy analysis can be improved by combining object-recognition with pixel-intensity-correlation. *Biotechnol J* 12. <https://doi.org/10.1002/biot.201600332>
- Mukherjee M, deRiso J, Otterpohl K et al (2019) Endogenous Notch Signaling in Adult Kidneys Maintains Segment-Specific Epithelial Cell Types of the Distal Tubules and Collecting Ducts to Ensure Water Homeostasis. *J Am Soc Nephrol* 30:110–126. <https://doi.org/10.1681/asn.2018040440>
- Muto S (2001) Potassium transport in the mammalian collecting duct. *Physiol Rev* 81:85–116
- O'Neil RG, Hayhurst RA (1985) Functional differentiation of cell types of cortical collecting duct. *Am. J. Physiol. - Ren. Fluid Electrolyte Physiol.* 17
- Palatini P (2012) Glomerular hyperfiltration: a marker of early renal damage in pre-diabetes and pre-hypertension. *Nephrol Dial Transplant* 27:1708–1714
- Pearce D, Soundararajan R, Trimpert C et al (2015) Collecting duct principal cell transport processes and their regulation. *Clin J Am Soc Nephrol* 10:135–146. <https://doi.org/10.2215/CJN.05760513>
- Pérez-Sánchez G, Jiménez A, Quezada-Ramírez MA et al (2018) Annexin A1, Annexin A2, and Dyrk 1B are upregulated during GAS1-induced cell cycle arrest. *J Cell Physiol* 233:4166–4182. <https://doi.org/10.1002/jcp.26226>
- Ramkumar N, Stuart D, Rees S et al (2014) Collecting Duct-Specific knockout of renin attenuates angiotensin II-Induced hypertension. *Am J Physiol - Ren Physiol* 307:F931–F938. <https://doi.org/10.1152/ajprenal.00367.2014>
- Ren YA, Liu Z, Mullany LK et al (2016) Growth Arrest Specific-1 (GAS1) Is a C/EBP Target Gene That Functions in Ovation and Corpus Luteum Formation in Mice. *Biol Reprod* 94:44. <https://doi.org/10.1095/biolreprod.115.133058>
- Reyes JL, Lamas M, Martin D et al (2002) The renal segmental distribution of claudins changes with development. *Kidney Int* 62:476–487. <https://doi.org/10.1046/j.1523-1755.2002.00479.x>
- Reyes JL, Nava E, Namorado MC (1992) Receptor-mediated effect of a synthetic thromboxane-analogue on cytosolic calcium in isolated proximal tubules. *Prostaglandins* 44:145–154. [https://doi.org/10.1016/0090-6980\(92\)90076-6](https://doi.org/10.1016/0090-6980(92)90076-6)
- Rincon-Choles H, Kasinath BS, Gorin Y, Abboud HE (2003) Angiotensin II and growth factors in the pathogenesis of diabetic nephropathy. *Kidney Int* 62:S8–S11. <https://doi.org/10.1046/j.1523-1755.62.s82.3.x>
- Romero-Trejo D, Mejía-Rodríguez R, Sierra-Mondragón E, Navarrete A, Pérez-Tapia M, González RO, Segovia J (2021) The systemic administration of neural stem cells expressing an inducible and soluble form of growth arrest specific 1 inhibits mammary gland tumor growth and the formation of metastases. *Cytotherapy* 23(3):223–235. <https://doi.org/10.1016/j.jcyt.2020.09.011>
- Rosas-Martínez L, Rodríguez-Muñoz R, del Namorado-Tonix M et al (2021) Hyperglycemic levels in early stage of diabetic nephropathy affect differentially renal expression of claudins-2 and -5 by oxidative stress. *Life Sci* 268. <https://doi.org/10.1016/j.lfs.2020.119003>
- Roy A, Al-Bataineh MM, Pastor-Soler NM (2015) Collecting duct intercalated cell function and regulation. *Clin J Am Soc Nephrol* 10:305–324. <https://doi.org/10.2215/CJN.08880914>
- Sacilotto N, Castillo J, Riffo-Campos ÁL et al (2015) Growth arrest specific 1 (Gas1) gene overexpression in liver reduces the in vivo progression of murine hepatocellular carcinoma and partially restores gene expression levels. *PLoS ONE* 10. <https://doi.org/10.1371/journal.pone.0132477>
- Segovia J, Zarco N (2014) Gas1 is a pleiotropic regulator of cellular functions: from embryonic development to molecular actions in cancer gene therapy. *Mini Rev Med Chem* 14:1139–1147
- Sierra-Mondragón E, Molina-Jijón E, Namorado-Tonix C et al (2018) All-trans retinoic acid ameliorates inflammatory response mediated by TLR4/NF-κB during initiation of diabetic nephropathy. *J Nutr Biochem* 60:47–60. <https://doi.org/10.1016/j.jnutbio.2018.06.002>
- Sierra-Mondragón E, Molina-Jijón E, Namorado-Tonix C et al (2018) Data on nephroprotective effect of all-trans retinoic acid in early diabetic nephropathy. *Data Br* 20:784–789. <https://doi.org/10.1016/j.dib.2018.08.080>
- Siragy HM, Awad A, Abadir P, Webb R (2003) The angiotensin II type 1 receptor mediates renal interstitial content of tumor necrosis factor-α in diabetic rats. In: *Endocrinology*. pp 2229–2233
- Stebel M, Vatta P, Ruaro ME et al (2000) The growth suppressing gas1 product is a GPI-linked protein. *FEBS Lett* 481:152–158. [https://doi.org/10.1016/S0014-5793\(00\)02004-4](https://doi.org/10.1016/S0014-5793(00)02004-4)
- Trepiccione F, Capasso G, Nielsen S, Christensen BM (2013) Evaluation of cellular plasticity in the collecting duct during recovery from lithium-induced nephrogenic diabetes insipidus. *Am J Physiol Physiol* 305:F919–F929. <https://doi.org/10.1152/ajprenal.00152.2012>
- Trevisan R, Dodesini AR (2017) The Hyperfiltering Kidney in Diabetes. *Nephron* 136:277–280
- van Roeyen CRC, Zok S, Pruessmeyer J et al (2013) Growth arrest-specific protein 1 is a novel endogenous inhibitor of glomerular cell activation and proliferation. *Kidney Int* 83:251–263. <https://doi.org/10.1038/ki.2012.400>
- Wagner CA, Finberg KE, Breton S et al (2004) Renal vacuolar H⁺-ATPase. *Physiol Rev* 84:1263–1314
- Wang H, Zhou X, Zhang Y et al (2012) Growth arrest-specific gene 1 is downregulated and inhibits tumor growth in gastric cancer. *FEBS J* 279:3652–3664. <https://doi.org/10.1111/j.1742-4658.2012.08726.x>
- Wang S, Mitu GM, Hirschberg R (2008) Osmotic polyuria: An overlooked mechanism in diabetic nephropathy. *Nephrol Dial Transplant* 23:2167–2172
- Wu H, Chen L, Zhou Q et al (2013) Aqp2-Expressing Cells Give Rise to Renal Intercalated Cells. *J Am Soc Nephrol* 24:243–252. <https://doi.org/10.1681/ASN.2012080866>
- Zamorano A, Lamas M, Vergara P et al (2003) Transcriptionally mediated gene targeting of gas1 to glioma cells elicits growth arrest and apoptosis. *J Neurosci Res* 71:256–263. <https://doi.org/10.1002/jnr.10461>
- Zamorano A, Mellström B, Vergara P et al (2004) Glial-specific retrovirally mediated gas1 gene expression induces glioma cell apoptosis and inhibits tumor growth in vivo. *Neurobiol Dis* 15:483–491. <https://doi.org/10.1016/j.nbd.2003.11.022>
- Zarco N, González-Ramírez R, González RO, Segovia J (2012) GAS1 induces cell death through an intrinsic apoptotic pathway. *Apoptosis* 17:627–635. <https://doi.org/10.1007/s10495-011-0696-8>
- Zhang L, He S, Guo S et al (2014) Down-regulation of miR-34a alleviates mesangial proliferation in vitro and glomerular hypertrophy in early diabetic nephropathy mice by targeting GAS1. *J Diabetes Complications* 28:259–264. <https://doi.org/10.1016/j.jdiacomp.2014.01.002>

Springer Nature or its licensor holds exclusive rights to this article under a publishing agreement with the author(s) or other rightsholder(s); author self-archiving of the accepted manuscript version of this article

is solely governed by the terms of such publishing agreement and applicable law.